To be presented at the Specialists Meeting on "Alloy Design For Fatigue and Fracture Resistance", 40th Meeting of the Structures and Materials Panel, Brussels, Belgium, April 14-15, 1975

LBL-3595

FUNDAMENTAL CONSIDERATIONS IN THE DESIGN OF FERROUS ALLOYS

Victor F. Zackay

February, 1975

Prepared for the U. S. Atomic Energy Commission
under Contract W-7405-ENG-48

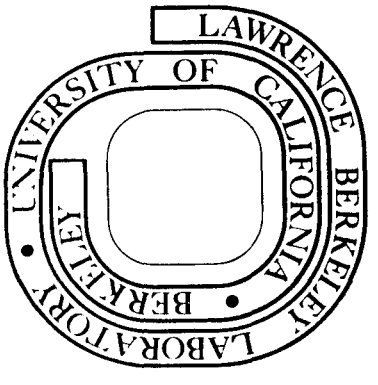

LBL-3595

c. 1

DISCLAIMER

FUNDAMENTAL CONSIDERATIONS IN THE DESIGN OF FERROUS ALLOYS

by
Victor F. Zackay
Inorganic Materials Research Division, Lawrence Berkeley Laboratory and
Department of Materials Science and Engineering, College of Engineering;
University of California, Berkeley, California 94720

INTRODUCTION

For more than a millennium, man has pondered the mysteries of making and using iron and its principal alloy--steel. Understanding has come slowly and, even today, in an era of scientific enlightenment the questions outnumber the answers and much mystery remains. This is particularly true in the field of alloy design-hard won experience and empiricism still dominate the synthesis of "new" steels. It is instructive to ask why this is so and whether this situation is likely to persist. If, indeed, it does, then the performance of new and sophisticated hardware will continue to be hampered by the limitations of empirically developed and, therefore, poorly understood, structural steels. Fortunately, the outlook is not this grim and the future holds much promise.

The metallurgist must draw upon diverse skills, invoke the art created by his innumerable predecessors, and tap the fundamental knowledge of numerous disciplines. Thus, with the aid of fundamental knowledge from the materials scientist, with the cooperation of the designer who stipulates the desired properties, and with the assistance of the process engineer who must produce the alloy on a large scale, the metallurgist formulates the composition and, lastly, prescribes the heat treatments which will endow the alloy with the requisite characteristics. It is these last and most critical steps that determine the success or failure of the alloy design effort. Success is totally dependent on (1) a working knowledge of the relationships between structure (defect structure and microstructure) and the mechanical properties of engineering interest and (2) a thorough comprehension of the solid state chemistry (alloy theory, thermodynamics and kinetics) of complex systems.

A lack of quantitative information in either of these two fields of knowledge will inevitably result in either complete failure or, at best, modest incremental improvements. Recognition of this situation some years ago led the author and his colleagues to confine their major research efforts in alloy design to two principal areas, i.e., (1) structure-property relationships and (2) a single aspect of solid state chemistry, viz., the isothermal kinetics of phase transformations in multicomponent iron-base systems. The following discussion is a brief summary of some of this research and is largely taken from a recently published[1] and an unpublished report[2] by the author and his collaborators.

I. QUENCHED AND TEMPERED STEELS

A principal objective in our research was to identify and characterize those elements of defect structure and microstructure in ultra high strength steels that influenced the plane strain fracture toughness. It was surmised that some elements of structure would enhance, while others would degrade, the fracture toughness. In the planning phases of this program it was assumed that weak or brittle microconstituents would degrade fracture toughness while others might prove beneficial. For example, the lamellar or plate-like forms of ferrite and cementite could lead to low energy tearing and microcracking when they occur in pearlitic and upper bainitic microstructures. Similarly, the presence of both nonmetallic inclusions and undissolved brittle carbides was thought to be undesirable. Also, evidence suggested that twinned martensite plates, as opposed to untwinned plates or laths, were detrimental. On the beneficial side, there was speculation and some evidence that retained austenite might, under certain circumstances, improve the fracture toughness of high strength steels. Accordingly, a series of heat treatments was devised for both commercial and laboratory type steels with the objective of minimizing the deleterious compositional and structural features while maximizing the beneficial ones.

A critical phase in the heat treatment of any steel is the austenitizing step. During austenitization many compositional and structural changes occur and profoundly influence the final microstructure and its associated mechanical properties. For example, low austenitizing temperatures favor a small austenite grain size but may leave a large fraction of brittle undissolved carbides. Conversely, high austenitizing temperatures lead to dissolution of a greater proportion of such carbides but cause a concomitant increase in austenite grain size. The complex and often unpredictable net effect of using a particular austenitizing temperature led, therefore, to a detailed study of its influence on the strength and toughness of a number of commercial and laboratory-type steels.

A. Austenitizing Temperature and Undissolved Alloy Carbides

As previously suggested, the presence of large undissolved particles of alloy carbides is likely to result in a deterioration of fracture toughness. The volume fraction and size of undissolved carbides left in the austenitic matrix prior to quenching, for a given composition, varies inversely with the austenitizing temperature. In an effort to evaluate relationships between austenitizing temperature, volume fraction of undissolved carbides, fracture toughness, and strength, several laboratory-type secondary hardening steels were studied. Their compositions are shown in Table I.

The effect of varying the austenitizing temperature on the room temperature yield strength, ultimate strength and the fracture toughness of as-quenched 0.30C-5Mo and 0.41C-5Mo steels[3] is shown in Fig. 1. In general, both strength and fracture toughness increased with increase in the austenitizing temperature. The increase in fracture toughness with austenitizing temperature for the lower carbon steel was particularly striking. Metallographic examination of these high molybdenum steels indicated that extensive solution of alloy carbides occurred above a critical austenitizing temperature. The fracture toughness was observed to increase markedly in the same temperature range. Associated with the increased solution of carbides and the improved fracture toughness was, as expected, a pronounced increase in grain size. Similar experiments were performed with another set of lower alloy steels in which complete dissolution of carbides

could be effected at austenitizing temperatures as low as 870°C. In this instance the fracture toughness of either steel was relatively independent of the austenitizing temperature (or grain size) as shown in Fig. 2.

Transmission electron microscopic studies using carbon replicas indicated that an austenitizing temperature of 870°C left undissolved carbides of approximately 0.05 microns in diameter for a 0.32C-2Mo steel, and of 1-3 microns for the 0.30C-5Mo steel, as shown in Figures 3 and 4, respectively. The deleterious effects of the larger carbides was suggested by the values of the ratio of plane strain fracture toughness to yield strength for the two steels in the as-quenched conditions. These were 0.42 for the 0.32C-2Mo steel and 0.27 for the 0.30C-5Mo steel. Furthermore, the ratios were equal for the 0.32C-2Mo steel austenitized at 870°C and the 0.30C-5Mo steel austenitized at 1200°C. These results strongly indicated that the presence of hard, brittle undissolved particles above a certain critical size could lead to a significant degradation of the fracture toughness of alloy steels. The results also suggest that the fracture toughness was insensitive to large variations in prior austenite grain size for those alloy steels whose matrix was free of undissolved carbides of sizes above a critical value. Additional information on these steels is found in the investigations of Goolsby[4] and T. Tom[3].

B. Austenitizing Temperature and Hardenability

The foregoing discussion showed that using relatively high austenitizing temperatures dissolved a greater proportion of alloy carbides and, this was usually associated with a large increase in prior austenitic grain size. Both the above phenomena tend to increase hardenability, i.e., either a thicker section can be through-hardened for a given quenching rate, or alternatively, a slower quenching rate may be used for a given section size without encountering the usual undesirable microstructural effects of metastable austenite decomposition. Austenitizing temperatures higher than those conventionally employed may therefore be used: (1) to enhance the hardenability of low alloy steels, and (2) to promote the presence of desirable phases for enhanced fracture toughness, such as retained austenite. An example of each of these possibilities is discussed in the following section (see also Katz.[5,6])

The room temperature plane strain fracture toughness of a relatively low hardenability steel, AISI 4130, is shown in Fig. 5 as a function of tempering temperature for several austenitizing treatments. (The tempering response of this steel and others as a function of austenitizing temperature is discussed in a subsequent section.) The plane strain fracture toughness of the as-quenched steel varies markedly with austenitizing temperature and severity of quench. An austenitizing temperature of 1200°C followed by an ice-brine quench and refrigeration in liquid nitrogen (IBQLN) resulted in nearly a two-fold increase in room temperature fracture toughness compared to that obtained by the conventionally recommended heat treatment of austenitizing at 870°C and oil quenching. A somewhat slower quench from 1200°C, i.e., oil quench *vs.* ice-brine, also improved the toughness relative to the commercial heat treatment but not as much as the more severe quench. Associated with the increases in fracture toughness were corresponding microstructural changes, as shown in Fig. 6 (a) and (b). The microstructure of a fracture toughness specimen oil quenched from 870°C consisted of a mixture of blocky ferrite and martensite, as shown in Fig. 6 (a). Extensive transmission electron microscopy using thin foils revealed that some of the martensite was autotempered. The microstructural appearance of a specimen ice-brine quenched from 1200°C was quite different, viz., there was virtually no evidence of ferrite, as shown in Fig. 6 (b). A similar correspondence between heat treatment, fracture toughness and microstructure existed for steel AISI 4330. Plots of plain strain fracture toughness *vs.* tempering temperature for two austenitizing treatments are shown in Fig. 7. Additional information on these steels is found in the investigations of Wood *et al.*[7]

Unconventional heat treatments of the kind described above for steels of high hardenability resulted in similar improvements in fracture toughness even though there appeared to be no corresponding microstructural changes except the expected grain size differences, as determined by optical metallographic observations. The room temperature plane strain fracture toughness of AISI 4340 steel is plotted in Fig. 8 as a function of tempering temperature for two austenitizing treatments. The preferred heat treatment involves a step-quench from 1200°C to 870°C followed by an oil quench. Quench cracking occurred in the steel when it was quenched from the higher temperature or if a quench more drastic than oil was used. As can be seen from Fig. 8 the plane strain fracture toughness of the as-quenched steel was nearly doubled by the step-quench heat treatment. Examination of the microstructures by transmission electron microscopy of specimens given both types of heat treatment revealed differences in the amount of retained austenite and in the nature of the substructure. As shown in the bright and dark field transmission micrographs of the specimen conventionally heat treated, the amount of retained austenite (revealed by use of an austenite reflection) was small, (shown in Fig. 9 (a) and (b)). In contrast, the same metallographic technique revealed extensive networks of retained austenite -- in some areas of the specimen almost every martensite plate and lath was surrounded by austenite films that were 100-200 Å thick, as shown in Fig. 10 (a) and (b) for the step quench treatment.

Transmission electron microscopy revealed another distinct microstructural difference between specimens given the two heat treatments. The packets of lath martensite were very similar for both austenitizing treatments. However, twinned martensite plates were observed in the conventional treatment only; the use of the step-austenitizing treatment apparently resulted in the virtual elimination of twinned martensite plates, as shown in a comparison of Figs. 11 (a) and (b). A detailed discussion of the role of these various changes in the microstructure and their possible effects on fracture toughness is found in a paper by Lai *et al.*[8] Briefly, it appears that both the presence of retained austenite, especially in the observed morphology, and the absence of twinned martensite plates favor the fracture toughness of specimens given the step-austenitizing heat treatment. Webster[9,10] and Antolovich *et al.*[11] have suggested that retained austenite may enhance the fracture toughness of high strength steels by either blunting an advancing crack or by undergoing a strain-or stress-induced transformation at the advancing crack tip. The consequences of the latter have been considered by Gerberich *et al.*[12], Antolovich and Singh[13] and, by Zackay *et al.*[14] Das and Thomas[15], Thomas[16] and, Thomas and Das[17] have comprehensively treated the problem of twinned martensite plates as they influence the fracture toughness of ultra-high strength steels. With the existing information, it is not possible to establish the individual or combined role of these microstructural features on the fracture toughness of complex high strength steels. The need for definitive solutions of these and other problems in the design of new and superior steels is discussed in a later section.

C. Austenitizing Temperature and Tempering Response

In the foregoing discussion, attention was centered on the effects that variations in the austenitizing temperature can have on the plane strain fracture toughness of as-quenched steels. It was shown that these effects, whether beneficial or detrimental, could usually be traced to the appearance or disappearance of some element of microstructure or substructure. The same can be said of the tempering response, although the causal relationships are less clear and are dependent in some cases upon subtle combined chemical and mechanical effects which appear to take place on a sub-microscopic scale.

The influence of tempering with variations in austenitizing temperature and severity of quench was shown earlier for several commercial steels, viz., Fig. 5 for AISI 4130 steel, Fig. 7 for AISI 4330 steel, and Fig. 8 for AISI 4340 steel. The chemical composition of these steels and one other --- the 300-M steel, are shown in Table II. The last mentioned steel is a modified version of AISI 4340 steel containing 0.08% vanadium and 1.59% silicon. A comparison of Figures 5, 7 and 8 reveal that the use of higher austenitizing temperatures resulted in tempered martensite embrittlement for the AISI 4130 and 4340 steels in the tempering range of 200-350°C. This type of embrittlement was not observed for the AISI 4330 and 300-M (not shown in the figures) steels treated at the high austenitizing temperature or for any of the steels conventionally heat treated. The fracture of the embrittled specimens was intergranular along prior austenite grain boundaries, while that of unembrittled specimens (either in the as-quenched condition or tempered at 200°C) occurred by dimpled rupture. No significant microstructural differences could be detected by transmission electron microscopy between the embrittled and the unembrittled specimens. The only compositional differences between the embrittled and unembrittled steels was the presence of vanadium and a larger amount of silicon in the latter. Several possible causes of the observed change in fracture mode have been discussed in detail by Lai et al.[8] One of the possible mechanisms for this type of embrittlement is the presence of certain impurity elements as suggested by Capus and Mayer[18], Low[19], Kula and Anctil[20], and Ohtani et al.[21], among others. Kula and Anctil[20] suggest that when cementite grows at prior austenite grain boundaries during tempering, such impurity elements as phosphorus, which are probably more soluble in ferrite than in cementite, will diffuse out of the cementite into the surrounding ferrite. A film of segregated impurities might build up at the interface between ferrite and cementite. The presence of the film may then result in a lowering of the interfacial energy and provide a low-energy path for intergranular fracture. Ohtani et al.[21] have suggested a similar mechanism for temper-embrittlement. These workers contend that the classic equilibrium segregation theory of temper embrittlement may have to be discarded. In accordance with their model, stabilization of carbides by elements such as molybdenum or vanadium is a possible way of suppressing embrittlement. The experimental results presented in this section on the tempering response of vanadium-containing and vanadium-free commercial steels subjected to high austenitizing temperatures are therefore not inconsistent with the Kula and Anctil model for tempered martensite embrittlement.

In a study of the role of impurity elements (P, S, Cu, As, Sn) on the critical flaw size for catastrophic fracture, Cottrell[22] stressed the importance of impurities. For example, the combined effect of As and S in degrading fracture toughness was far greater than the sum of their individual effects. As might be expected, the most serious deterioration of toughness was observed at a tempering temperature when both temper embrittlement (dependent on tempering temperature) and sulfide embrittlement (largely independent of tempering temperature) occurred.

It is clear from these and many other studies that the type and the level of impurities have a major influence on the plane strain fracture toughness of ultra-high strength steels. As Cottrell points out in his paper,[22] the effect of purification on the critical defect size in a conventional low alloy steel with a yield strength of 240,000 psi, may be far greater than that achieved by the alternative route of the substitution of the low alloy steel with a maraging steel. Darmara[23] has reviewed some then current and proposed methods of purifying steel. It is obvious from his remarks that the steel-making processes of the future will produce steels with combinations of mechanical properties that are achieved now only in the controlled purity alloys of the research laboratory.

D. An important Unsolved Problem

The alloying elements of steel and the solid state reactions which they undergo determine the structure and, therefore, the properties of steel. The complex nature of these reactions is not yet fully understood and understanding the nature of these reactions is important in the economic design of superior steels. For example, even if the influences of all the common alloying elements on the thermodynamics and kinetics of the principal isothermal reactions of plain carbon steels were individually known, the information would be insufficient for the effective design of complex steels because commercial steels contain many interacting elements whose total effect is often different from that predicted on the basis of the individual elements alone. A real need exists therefore for a technique for rapidly predicting the single and the combined effects of all the common alloying elements on the solid state metallurgical reactions that are important in the heat treatment of steel. Knowing the initiation (incubation) and finish times of these reactions and their associated kinetics is particularly important. Progress made in the authors' laboratory in developing such a technique is described below.

The rapid method of studying isothermal reactions in steels consists in quenching the steel sample from the austenitizing temperature to a subcritical temperature in an isothermal bath and holding it within the magnetic field of an inductor coil. The increase in permeability accompanying austenite decomposition increases the inductance of the coil, and this changes the resonant frequency of the cricuit. An automatic continuous recording of the corresponding period provides a convenient and accurate method for following the austenite decomposition. Quantitative information on austenite decomposition kinetics can be obtained within two seconds after the start of quenching (Babu et al.,[24] and Ericsson et al.[25]). An example illustrating some of the preliminary results obtained by this method is described below.

In the recently reported T-T-T diagrams for AISI 4340 steel, the bainite range is shown as a smooth C-shaped curve, Fig. 12(a). Investigations by the new method showed significant differences in the shape and character of the lower bainite region. As shown in Fig. 12(b), the incubation period for the formation of lower bainite decreased at temperatures just above the M_s and gave an S-shaped curve for the bainite

reaction. This acceleration of austenite decomposition at temperatures just above M_s has been observed previously (Howard and Cohen,[26] Schaaber,[27] and Radcliffe and Rollason[28]).

That part of the lower bainite curve which extended below the M_s had a C-shape, as shown in Fig. 12(b). Immediately below the M_s, the bainite reaction began almost instantly after the end of the martensite reaction. This rapid onset at temperatures just below the M_s is well established in the literature and is associated with the increased nucleation of the bainite reaction by the strain effects associated with the austenite to martensite transformation. The decreased rate of bainite formation at temperatures well below the M_s was apparently due to the lower diffusion rates of carbon.

The element silicon is known to affect the kinetics of tempering[29-32] as well as the mechanical properties of tempered martensite steels.[33, 34] The reasons for this behavior are not known, but speculation has centered on the retardation of the nucleation of iron-carbide by silicon[30, 34] as well as its well known influence on the thermodynamic activity of carbon.[35] The experimental observations and the associated theoretical speculations suggest that silicon might have a significant influence on the isothermal formation of lower bainite from metastable austenite.

The low temperature portion of a T-T-T diagram of AISI 4340 steel with 3.0% added silicon is shown in Figure 13. (The standard alloy contains about 0.25% silicon.) The effect of the added silicon on the kinetics of transformation is striking as can be seen easily from a comparison of Fig. 12 (b) and Fig. 13. The time for isothermal transformation of 50% of the austenite is about 20 minutes for the silicon modified 4340 steel as compared to a few hundred seconds for the standard 4340 steel. The morphology of the retained austenite in the silicon modified steel is clearly seen in the bright field - dark field pair of electron micrographs of Fig. 14. The dark field picture was taken using an austenite reflection. The retained austenite was present in the form of films decorating the lath boundaries of ferrite as shown at A, with some austenite regions with a thickness equal to the lath size of bainitic ferrite as seen at B. A pool of austenite can also be observed at C. It was possible to vary the amount of retained austenite over a wide range by changing the temperatures and times of isothermal decomposition.

Reactions of the type described above and their associated microstructures have meaning for both the user of existing commercial steels and the designer of new ones. To the user of commerical steels, the precise location and shape of the lower and upper bainite reaction curves is significant from a hardenability viewpoint. Avoiding certain cooling rates can prevent the formation of upper bainite, and undesirable microstructures for mechanical properties. This is especially important in complex parts with varying section sizes. To the designer of new steels, knowledge of the details of the lower bainite and martensite reactions presents an opportunity to evaluate the mechanical properties of steels with the unusual mixed microstructures of lower brainite, autotempered and tempered martensite, and retained austenite. This new experimental technique for the rapid determination of T-T-T diagrams, coupled with basic studies of austenite decomposition on simple high purity steels such as those, for example, of Aaronson and Domian[36] and Hehemann et al.,[37] could eventually provide the basis for designing complex steels that are both economical and superior in properties to those currently available. The mechanical properties of these steels, especially the strength, ductility and the fracture toughness, were most unusual and are discussed in the following sections.

E. Fracture Toughness of Quenched and Tempered Steels

As is predictable from the basic principles of materials science, low fracture toughness of quenched and tempered steel is associated with the presence of certain types of microstructural features. Sulfide inclusions act as microcrack nuclei and therefore induce macrofracture at relatively low strains in fracture toughness specimens. Similarly, carbide particles, undissolved during austenitizing, lower toughness. Free ferrite, whether present as separate grains or as platelets in upper bainite in ultra-high-strength steels, lowers fracture toughness by a substantial amount.

Autotempered martensite (with no interlath carbides) formed during the quenching operation is tough. Lower bainite, and tempered martensite free from lath boundary films of carbides, are also tough and fracture resistant microstructural constituents. The presence of retained austenite films around autotempered laths of martensite adds substantially to the inherent toughness of the autotempered martensitic structure. The substructure of martensite itself is also important, e.g. transformation twinning in carbon steels lowers toughness.[38]

Figure 15 summarizes the results of tests on steels that had been given the 1200°C austenitizing treatment. The fracture toughness, K_{IC}, is plotted against the yield strength. In this figure there are two bands which show the ranges of yield strength and fracture toughness values reported in the literature for commercial AISI 4340 steel and the 18 Ni maraging alloy. The maraging steels are usually considered to have the highest value of plane strain fracture toughness obtainable at a given yield strength. The circles are test points for steel given special heat treatments described herein. The toughness values have been moved out of the lower and into the upper band. Furthermore, there are theoretical reasons to believe that fracture toughnesses well above the maraging steel band can be obtained with quenched and tempered steels through modifications of chemical composition and thermal treatments.

Figure 16 shows the approximate range of results obtained with TRIP steels,[12, 13, 39, 40] and how the fracture toughness values compare with those of quenched and tempered, and maraging steels. The TRIP steels are metastable austenitic ultra-high-strength steels that transform martensitically when plastically deformed. These steels contain 0.3% carbon or more, and the strain-induced martensite formation provides an additional strengthening mechanism. A volume increase of approximately 3% (corresponding to a linear change of 1%) is associated with the austenite to martensite transformation. The transformation strains augment the ductility and add to the fracture toughness. The volumetric expansion tends to reduce the three-dimensional tensile stresses that are developed during plastic straining near the apex of a notch. This changes the stress state toward a condition which favors a more ductile performance of a fracture toughness specimen. Antolovich and Singh[13] have recently measured the fracture toughness (K_{IC}) of a TRIP steel having a yield strength of 250,000 psi. As these authors point out, their

value (95 ksi in.$^{1/2}$) may be low as the steel had a relatively high carbon content, viz., 0.6%. The fracture toughness is likely to be low for high carbon TRIP steel because the strain - induced untempered martensite provides crack paths. If, however, their value is representative of TRIP steels, then it appears highly probable that compositions and heat treatments can be formulated for low alloy steels whose plain strain fracture toughnesses will be as high (or nearly so) as those of the toughest laboratory-type ultra-high-strength steels ever made, as suggested by the summary plot shown in Fig. 17. (For additional details see References 3, 8, 41-44.)

F. Fracture Toughness of Silicon Modified Steels Given an Isothermal Hold

In a previous section, mention was made of the unusual microstructures which could be obtained by interposing an isothermal hold between the austenitizing treatment and the quench. The structure-property relationships of a 300M steel given heat treatments of this kind are interesting and, in some instances, rather unexpected.

In this study, different time-temperature paths were devised which result in mixed microstructures having various combinations of retained austenite, upper bainite, lower bainite and tempered lath and plate martensites. Several tentative conclusions can be reached regarding the desirable and undesirable combinations of these microconstituents.

The combination of strength and toughness of 300M steel was significantly improved, over that obtained with the conventional heat treatment, by the superposition of an isothermal hold (prior to quenching) at a temperature just below the M_s. After quenching and tempering the microstructure consisted of a mixture of tempered lath martensite, lower bainite and retained austenite. The properties associated with this microstructure were equivalent in fracture toughness to that of a maraging steel with an ultimate tensile strength of 280,000 psi.

An unexpected result was the behavior of specimens whose heat treatment resulted in a microstructure composed of upper bainite, tempered plate martensite and retained austenite. The presence of either upper bainite and/or tempered plate martensite is usually considered to be highly deleterious to the fracture toughness of ultra-high-strength steels. However, the combination of strength and toughness of these steels were comparable to those of maraging steels. Maraging-type properties were observed over a range of tensile strengths from 220,000 to 260,000 psi. These preliminary results suggest that the detrimental effects of some microconstituents can be largely off-set by the presence of a beneficial one, namely, retained austenite of the appropriate stability, morphology and volume fraction.

II. EXPLORATORY STUDIES OF CARBON-FREE FERROUS ALLOYS

A vigorous part of our research effort for the past decade has been on iron-base systems with carbon as the principal alloying element. In the past several years, however, some exploratory studies have been made of carbon-free alloys which utilize intermetallic compounds as dispersion hardening agents rather than the usual transition metal carbides. The studies are part of a long range effort to establish the principles of alloy design of non-carbon containing ferrous systems for cryogenic,[1, 2, 45-48] room temperature[49] and elevated temperature service.[50-52] Potentially useful solid state transformations and their kinetics have been stressed, rather than the development of practical alloy systems, in these investigations.

A. Some Design Features for Cryogenic Alloys

In the design of BCC iron alloys for cryogenic service the problems are both chemical and microstructural. For maximum toughness at low temperatures the BCC matrix must be purged as free as possible of embrittling interstitials. This can be accomplished by the use of liquid and solid state scavenging techniques. The elements Ti and Al when used together in small amounts and in the appropriate ratio are exceptionally effective as solid state scavengers. A further and necessary decrease of the ductile-to-brittle transition temperature can be achieved by a drastic reduction of grain size - a reduction which cannot be accomplished by the more conventional techniques of recrystallization. The required grain size can be obtained by cycling through a phase transformation.

The temperature of the α to γ phase transformation in alloys of iron is largely established by the solute content; in the present instance the element nickel is utilized. Optimally, it is desirable to have this temperature below that of rapid grain growth and, for efficient nucleation, in the two phase (α plus γ) region. The charpy V-notch impact energy, at -196°C, is shown in Fig. 18, as a function of reheat temperature in the two phase region. The data given are for specimens given either a one or a two cycle treatment and/or one which was cold-worked prior to reheating. The variation of impact energy at -196°C with refined prior austenite grain size is shown in Fig. 19. It was observed that there was a sharp drop of impact energy above a critical grain size of about 15 microns. Optimization of compositional and thermal-mechanical techniques such as those described above has enabled a colleague, Prof. J. W. Morris and his students, to produce specimens whose charpy V-notch values were over 200 ft-lbs. at the temperature of liquid helium. (For further details see Refs. 46-48.) As a natural extension of these cryogenic studies, alloys of the Fe-Ni-Ti system have been investigated in recent months by Dr. B. Francis of our laboratory,[49] with respect to their useful combinations of strength and toughness at room temperature.

B. Some Design Features for Room Temperature Alloys

The emergence of maraging-type alloys in the past decade has revealed the potential for carbon-free ferrous systems wherein the strengthening dispersoids are intermetallic compounds rather than transition metal carbides. The maraging-type system, Fe-Ni-Ti, is known to have attractive high strength potential but its exploitation has been hindered by the tendency of the strengthening dispersoid, Ni_3Ti, to form embrittling grain boundary networks. This is especially true for alloys containing a large volume fraction of compound--a desirable feature if ultra high strength is to be attained.

Our studies suggest that embrittlement in this system can possibly be minimized by the utilization of heat treatments which cause other competing grain boundry reactions to occur. For example, variations of the

aging temperature of Fe-Ni-Ti alloys can cause either austenite or precipitate to form at both the prior austenite grain boundaries and the martensite lath boundaries. The fracture toughness of Fe-Ni-Ti alloys, at strength levels up to about 200,000 psi, is largely determined by the degree of grain boundary embrittlement. The embrittlement is, in turn, dependent on the volume fraction and morphology of precipitate which forms in the grain boundaries. If austenite can be caused to form at the grain and lath boundaries, rather than the precipitate, the fracture mode is transgranular instead of intergranular and the combination of strength and toughness that can be realized is superior. Above yield strengths of about 200,000 psi in alloys with a higher ratio of titanium to nickel, the fracture mode becomes intergranular once again and the toughness falls. The reasons for this behavior are presently under investigation.

The rate of formation of austenite as a function of temperature was determined by means of a magnetic technique.[24] The percentage of austenite detected as a function of isothermal holding time is shown in Fig. 20(a). Also shown in Fig. 20(b) are the aging curves for the precipitation process. These aging curves were taken as an indirect measure of the rate of formation of the precipitate. In these alloys, the precipitate, hexagonal Ni_3Ti, does not appear to form in the austenite. For example, no precipitation was observed in the austenite regions in specimens aged at 650°C; precipitation was observed in the ferritic regions, and therefore, if appreciable austenite forms during the aging process either similtaneously with or before the production of the precipitate, the embrittlement might be expected to decrease, as was found to be the case.

At higher aging temperatures in the α plus γ region i.e., those which favor the formation of austenite, the toughness (K_{Ic}) is the highest for a given strength level, as shown in Table III. The converse is true for lower aging temperatures. At intermediate temperatures and times the situation is more complex. Current studies suggest there is a critical balance between austenite and precipitate formation under these conditions and that once a precipitate forms in the grain boundary further formation and growth of austenite is not particularly helpful. This does not appear to be the case for higher aging temperatures. The combination of strength and toughness achieved to date in an Fe-16Ni-1.5Ti alloy by the means described above is equivalent to that of a standard 200 grade maraging steel. The technique of utilizing competing grain boundary reactions appears, in this case, to be more significant than the particular composition of the alloys or the specific mechanical properties which were obtained. Further studies of this kind may be warranted in promising ferrous systems where grain boundary embrittlement is the limiting alloy design feature.

C. Ferrous Alloys for Elevated Temperature Use

A somewhat different approach than that mentioned in the preceding section was taken in the design of BCC ferrous alloys, strengthened by a Laves phase (Fe_2Ta) for moderately elevated temperature use.[50-52] In this instance, the morphology of the grain boundary embrittling phase was altered. The virtually continuous grain boundary film was spheroidized and thereby rendered discontinuous by a high temperature aging treatment within the γ + Fe_2Ta region. A representative alloy (nominal composition Fe - 7 at. pct Cr - 1 at. pct Ta-0.5 at. pct Mo) treated in this manner had a creep strength at 649°C equivalent to those of some of the best BCC ferrous alloys that are now commercially available.[51]

CONCLUDING REMARKS

There now exists, for ferrous alloys, a wealth of information on the cause and effect relations between the elements of microstructure and the fracture toughness. The relations were established from experimental rather than theoretical considerations. However, the observed structure vs. property correlations are in accord with what is presently known of the theories of defects in solids and of linear elastic fracture mechanics.

The fortunate state of affairs mentioned above is in all likelihood a natural consequence of the significant advancements that have been made in fields relevant to alloy design. Special mention should be made of, one, high resolution electron optical instrumentation for the identification and characterization of the elements of microstructure and, two, of the standardization and perfection of the techniques for the quantitative measurements of the fracture toughness of solids.

One of the major problems now confronting the designer of alloys is that of producing alloys having microstructures with the desirable microconstituents and without the undersirable ones. Solutions to these problems require a detailed and thorough knowledge of the interactions of elements in metallic solids as they influence the thermodynamics, kinetics and phase transformations of solids. For example, if retained austenite of a specific morphology and with a predetermined volume fraction and stability is desirable, then what must be the composition and the heat treatment of an alloy to produce such a microstructural configuration?

The answer to the above question (and innumerable ones like it) will bring the metallurgist nearer to his long sought goal - the establishment of a sound fundamental basis for the design of alloys.

REFERENCES

1. Zackay, V. F., Parker, E. R., Morris, J. W. Jr., Thomas, G. — Mat. Sci, and Eng., Vol. 16, 1974, 201.

2. Zackay, V. F., Parker, E. R. — Alloy Design, Tien, J. K., and Ansell, G. S., eds, Academic Press, New York, 1975. Also LBL-2782, 1974, Lawrence Berkeley Laboratory, Berkeley, California 97420.

3. Tom, T. — D. Eng. Thesis, LBL-1856, 1973, University of California, Berkeley, California 94720.

4. Goolsby, R. D. — Ph. D. Thesis, LBL-405, 1971, University of California, Berkeley, California 94720.

5. Katz, R. N. — Tech. Note WAL TN 320.1/8, Watertown Arsenal, Watertown, Mass., 1961.

6. Katz, R. N. — Tech. Note AMRA TN 65-09, Materials Engineering Division, U. S. Army Materials Research Agency, Watertown, Mass. 1965.

7. Wood, W. E., Parker, E. R., Zackay, V. F. — LBL-1474, 1973, Lawrence Berkeley Laboratory, Berkeley, California 94720.

8. Lai, G. Y., Wood, W. E., Parker, E. R., Zackay, V. F. — In preparation.

9. Webster, D. — Trans. ASM, Vol. 61, 1968, 816.

10. Webster, D. — Met. Trans., Vol. 2, 1971, 2097.

11. Antolovich, S. D., Saxena, A., Chanani, G. R. — Met. Trans., Vol. 5, 1974, 633.

12. Gerberich, W. W., Hemmings, P. L., Zackay, V. F. — Met. Trans., Vol. 2, 1971, 2243.

13. Antolovich, S. D., Singh, B. — Met. Trans., Vol. 2, 1971, 2135.

14. Zackay, V. F., Parker, E. R., Fahr, D., Busch, R. — Trans. ASM, Vol. 60, 1967, 252.

15. Das, S. K., Thomas, G. — Trans. ASM, Vol. 62, 1969, 659.

16. Thomas, G. — Met. Trans., Vol. 2, 1971, 2373.

17. Thomas, G., Das, S. K. — J. Iron Steel Inst., Vol. 209, 1971, 801.

18. Capus, J. M., Mayer, G. — Metallurgia, Vol. 62, 1960, 133.

19. Low, J. R., Jr. — Trans. Met. Soc. AIME, Vol. 245, 1969, 2481.

20. Kula, E. B., Anctil, A. A. — J. Mater., Vol. 4(4), 1969, 817.

21. Ohtani, H., Geng, H. C., McMahon, C. J., Jr. — Met. Trans., Vol. 5, 1974, 516.

22. Cottrell, C. L. M. — Fracture Toughness of High Strength Materials: Theory and Practices, ISI Publication 120, 1970. The Iron and Steel Institute, London, 112.

23. Darmara, F. N. — J. Metals, Vol. 19(12), 1967, 42.

24. Babu, B. N. P., Ott, D., Parker, E. R., Zackay, V. F. — LBL-2502, 1974, Lawrence Berkeley Laboratory, Berkeley, California 94720.

25. Ericsson, C. E., Parker, E. R., Zackay, V. F. — LBL-2762, 1974, Lawrence Berkeley Laboratory, Berkeley, California 97420.

26. Howard, R. T., Jr., Cohen, M. — Trans. AIME, Vol. 176, 1948, 384.

27. Schaaber, O. — Trans. AIME, Vol. 203, 1955, 559.

28. Radcliffe, S. V., Rollason, E. C. — J. Iron Steel Inst., Vol. 191, 1959, 56.

29. Allten, A. G., Payson, P. — Trans. ASM, Vol. 45, 1953, 498.

30. Owen, W. S. — Trans. ASM. Vol. 46, 1954, 812.

31. Keh, A. S., Leslie, W. C. — Materials Science Research, Vol. 1, Plenum Press, New York, 1963, 208.

32. Speich, G. R., Leslie, W. C. — Met. Trans., Vol. 3, 1972, 1043.

33. Shih, C. H., Averbach, B. L. Cohen, M. — Trans. ASM, Vol. 48, 1958, 86.

34. Altstetter, C. J., Cohen, M., Averbach, B. L. — Trans. ASM. Vol. 55, 1962, 287.

35. Wada, T., Wada, N., Elliot, J. F., Chipman, J. — Met. Trans., Vol. 3, 1972, 1657.

36. Aaronson, H. I., Domian, H. A. — Trans. Met. Soc. AIME, Vol. 236, 1966, 781.

37. Hehemann, R. F., Kinsman, K. R., Aaronson, H. I. — Met. Trans., Vol. 3, 1972, 1077.

38. Huang, D., Thomas, G. — Met. Trans., Vol. 2, 1971, 1587.

39. Gerberich, W. W., Hemmings, P. L., Merz, M. D., Zackay, V. F. — Trans. ASM. Vol. 61, 1968, 843.

40. Gerberich, W. W., Hemmings, P. L., Zackay, V. F., Parker, E. R. — Fracture 1969, Pratt, P. L., ed., Chapman and Hall, Ltd., London, 1969, 288.

41. Zackay, V. F., Parker, E. R., Goolsby, R. D., Wood, W. E. — Nature Phys. Sci., Vol. 236(68), 1972, 108.

42. Parker, E. R., Zackay, V. F. — Eng. Fr. Mech., Vol. 5, 1973, 147.

43. Zackay, V. F., Parker, E. R., Wood, W. E. — Microstructure and Design of Alloys, Inst. Metals, London, 1973, 175.

44. Wood, W. E., Parker, E. R., Zackay, V. F. — LBL-1474, 1973. Lawrence Berkeley Laboratory, Berkeley, California 94720.

45. Yokota, M. J., Sasaki, G., Horwood, W. A. — LBL-2278, 1974, Lawrence Berkeley Laboratory, Berkeley, California 94720.

46. Jin, S., Horwood, W. A., Morris, J. W., Jr., Zackay, V. F. — Advan. Cryog. Eng., Vol. 19, 1974, 373.

47. Jin, S., Morris, J. W., Jr., Zackay, V. F. — Advan. Cryog. Eng., Vol. 19, 1974, 379.

48. Jin, S. Morris, J. W., Jr., Zackay, V. F. — Presented at Materials Engineering Congress, Chicago, Illinois, October 1973.

49. Francis, B. — Ph. D. Thesis, LBL-1856, 1975, University of California, Berkeley, California 94720.

50. Zackay, V. F., Parker, E. R., Bhandarkar, D. — Proc. John E. Dorn Memorial Symp. on Rate Processes in Plastic Deformation, Cleveland, Ohio, October 1972. Also LBL-1174, 1972, Lawrence Berkeley Laboratory, Berkeley, California 94720.

51. Bhat, M. S. M. S. Thesis, LBL-2277, 1974, University of California, Berkeley, California 94720.

52, Bhandarkar, D., Bhat, M. S., Zackay, V. F., Parker, E. R. LBL-2573, 1974, Lawrence Berkeley Laboratory, Berkeley, California 94720.

ACKNOWLEDGEMENTS

The studies described above were done in close collaboration with my friend and co-worker, Prof. Earl R. Parker, whose counsel and constant encouragement are deeply appreciated.

The author is grateful to Drs. Michael Yokota, George Lai, William Wood, Thomas Tom, Naga Prakash Babu and Ben Francis for use of unpublished data, to Dr. Robert Ritchie for his critical technical review and, lastly, to Mr. M. S. Bhat for his valuable assistance in preparing this manuscript.

In the performance of this work I gratefully acknowledge the help and enthusiastic support of the United States Atomic Energy Commission through the Inorganic Materials Research Division of the Lawrence Berkeley Laboratory, Office of Naval Research, the Airforce Materials Laboratory and the Army Materials and Mechanics Research Center.

TABLE I

CHEMICAL COMPOSITIONS OF C-Mo STEELS

	Compositions, Wt. %					
Designations	C	Mo	Mn	S	P	Ni
0.32C-2Mo	0.32	1.96	0.65	0.005	0.007	--
0.30C-5Mo	0.30	5.03	0.60	0.005	0.008	--
0.41C-5Mo	0.41	4.93	0.51	0.005	0.007	--
0.35C-1Mo-3Ni	0.35	0.95	0.61	0.005	0.007	3.1

Sn, Sb < 0.002%, As < 0.005% and Si < 0.02% in all steels.

TABLE II

CHEMICAL COMPOSITION OF LOW ALLOY STEELS

	Compositions, Wt. %									
STEEL	C	Mn	Cr	Ni	Mo	S	Si	Cu	P	V
AISI 4130-A	0.31	0.57	0.85	0.15	0.18	0.009	0.28	0.21	0.008	<0.005
AISI 4130-B	0.33	0.63	0.90	0.15	0.18	0.009	0.27	0.19	0.008	<0.005
AISI 4330	0.28	1.02	0.85	1.80	0.40	0.005	0.28	0.10	0.009	0.07
AISI 4340	0.40	0.85	0.72	1.73	0.26	0.010	0.22	0.14	0.004	<0.005
300-M	0.41	0.79	0.75	1.85	0.43	0.002	1.59	0.04	0.008	0.08

TABLE III

TOUGHNESS OF ALLOY Fe-16Ni-1.5Ti FOR DIFFERENT AGING TEMPERATURES

Aging Temp.	R_c Hardness ($\sigma y \sim 200$ksi)	K_{IC} (ksi $\sqrt{in}$) (23°C)	CVN (ft-lbs) (23°C)
600°C	43	∿114	27
550°C	43	∿ 50	14
450°C	43	-	3

FIGURE CAPTIONS

Fig. 1 Plots showing the influence of austenitizing temperature on room temperature fracture toughness (K_{IC} or K_Q), yield strength (Y.S.), and ultimate strength (U.S.) of 0.30C-5Mo and 0.41C-5Mo steels.

Fig. 2. Plots of room temperature plane strain fracture toughness vs. prior austenite grain size (indicated by ASTM grain size number) for as-quenched 0.34C-1Mo and 0.35C-1Mo-3Ni steels.

Fig. 3. Transmission electron micrograph of a carbon replica showing fine undissolved carbides in as-quenched 0.32C-2Mo steel, austenitized at 870°C.

Fig. 4. Transmission electron micrograph of a carbon replica showing 1-3 micron size undissolved carbides in as-quenched 0.30C-5Mo steel, austenitized at 870°C.

Fig. 5. Plots of room temperature plane strain fracture toughness vs. tempering temperature for AISI 4130 steel. Austenitizing temperatures and quenching media are indicated.

Fig. 6. Microstructure of AISI 4130 steel: (a) austenitized at 870°C and oil quenched (arrows indicate ferrite and upper bainite), and (b) austenitized at 1200°C and ice-brine quenched.

Fig. 7. Plots of room temperature plane strain fracture toughness vs. tempering temperature for AISI 4330 steel. Austenitizing temperatures and quenching media are indicated.

Fig. 8. Plots of room temperature plane strain fracture toughness vs. tempering temperature for AISI 4340 steel. Austenitizing

temperatures and quenching media are indicated.

Fig. 9. Transmission electron micrographs of as-quenched AISI 4340 steel: (a) bright field and (b) dark field of austenite reflection for the 870°C austenitized specimen.

Fig. 10. Transmission electron micrographs of as-quenched AISI 4340 steel: (a) bright field and (b) dark field of an austenite reflection for the 1200°C → 870°C austenitized specimen.

Fig. 11. Transmission electron micrographs of martensite plates in AISI 4340 steel: (a) austenitized at 870°C, showing extensive fine transformation twins in a martensite plate marked P, (b) austenitized at 1200°C, showing absence of transformation twins and presence of ε carbides in a cross-hatched morphology in martensite plates marked P. A prior austenite grain boundary is marked GB.

Fig. 12. T-T-T diagrams of AISI 4340 steel: (a) as reported in the literature, and (b) as determined by the new magnetic permeability technique. (Only bainite and martensite ranges shown.)

Fig. 13. T-T-T diagram of 3% Si modified 4340 steel (only the bainite and martensite ranges are shown).

Fig. 14. Transmission electron micrographs of 3% Si modified 4340 steel: (a) bright field and (b) dark field of an austenite reflection. The steel was austenitized at 900°C and isothermally transformed at 307°C. Films of austenite decorate the lath boundaries of ferrite at A, with austenite regions with a thickness equal to the lath size of bainite ferrite at B, and a pool of austenite at C.

Fig. 15. Plots of fracture toughness, K_{IC}, vs. yield strength. The two shaded bands represent the range of values found in the literature for AISI 4340 and 18% Ni maraging steels. The circles are data points from the present investigation.

Fig. 15. Plots of fracture toughness vs. yield strength. Bands for commercial steels (K_{IC}) and metastable austenite TRIP steels (K_C).

Fig. 17 A summary plot of plane strain fracture toughness vs. yield strength. The band is for the 18% Ni maraging steel and the dotted line shows the trend for TRIP steels. The circles are data points from the present investigation for as-quenched and tempered 4340 steel.

Fig. 18. Plots of charpy V-notch impact energy at -196°C vs. reheating temperature for Fe-12Ni-0.5Ti alloy. The heat treatments are indicated.

Fig. 19. Relationship between prior austenite grain size and charpy impact energy at -196°C for the Fe-12Ni-0.5Ti alloy.

Fig. 20. Plots of (a) percent austenite vs. isothermal holding time and (b) hardness vs. isothermal holding time for the alloy Fe-16Ni-1.5Ti. The different isothermal holding temperature are indicated.

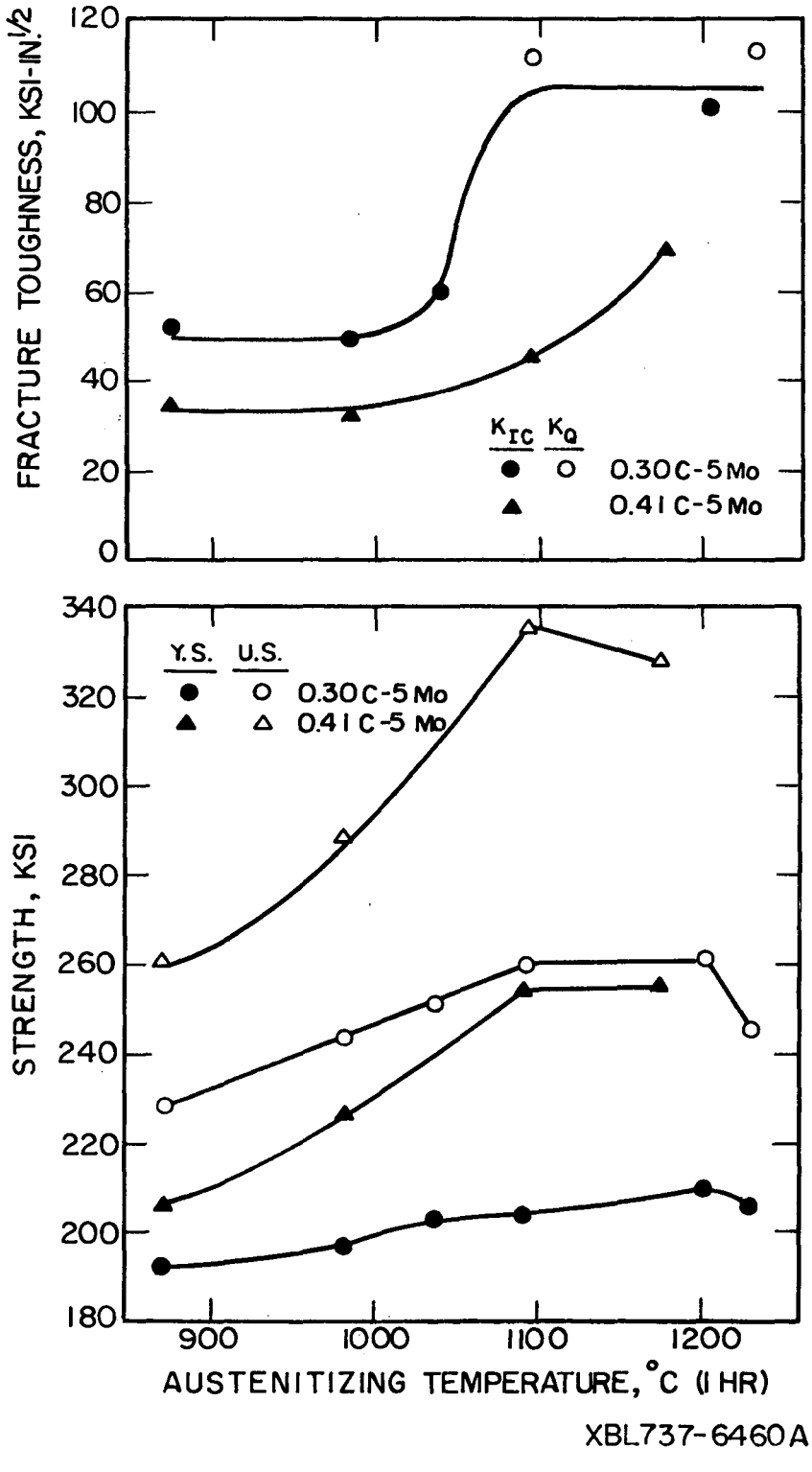
FRACTURE TOUGHNESS, KSI-IN.$^{1/2}$
120
100
80
60
40
20
0
K_{IC} K_Q
0.30C-5Mo
0.41C-5Mo
STRENGTH, KSI
340
320
300
280
260
240
220
200
180
Y.S. U.S.
0.30C-5Mo
0.41C-5Mo
900
1000
1100
1200
AUSTENITIZING TEMPERATURE, °C (1 HR)
XBL737-6460A

Fig. 1

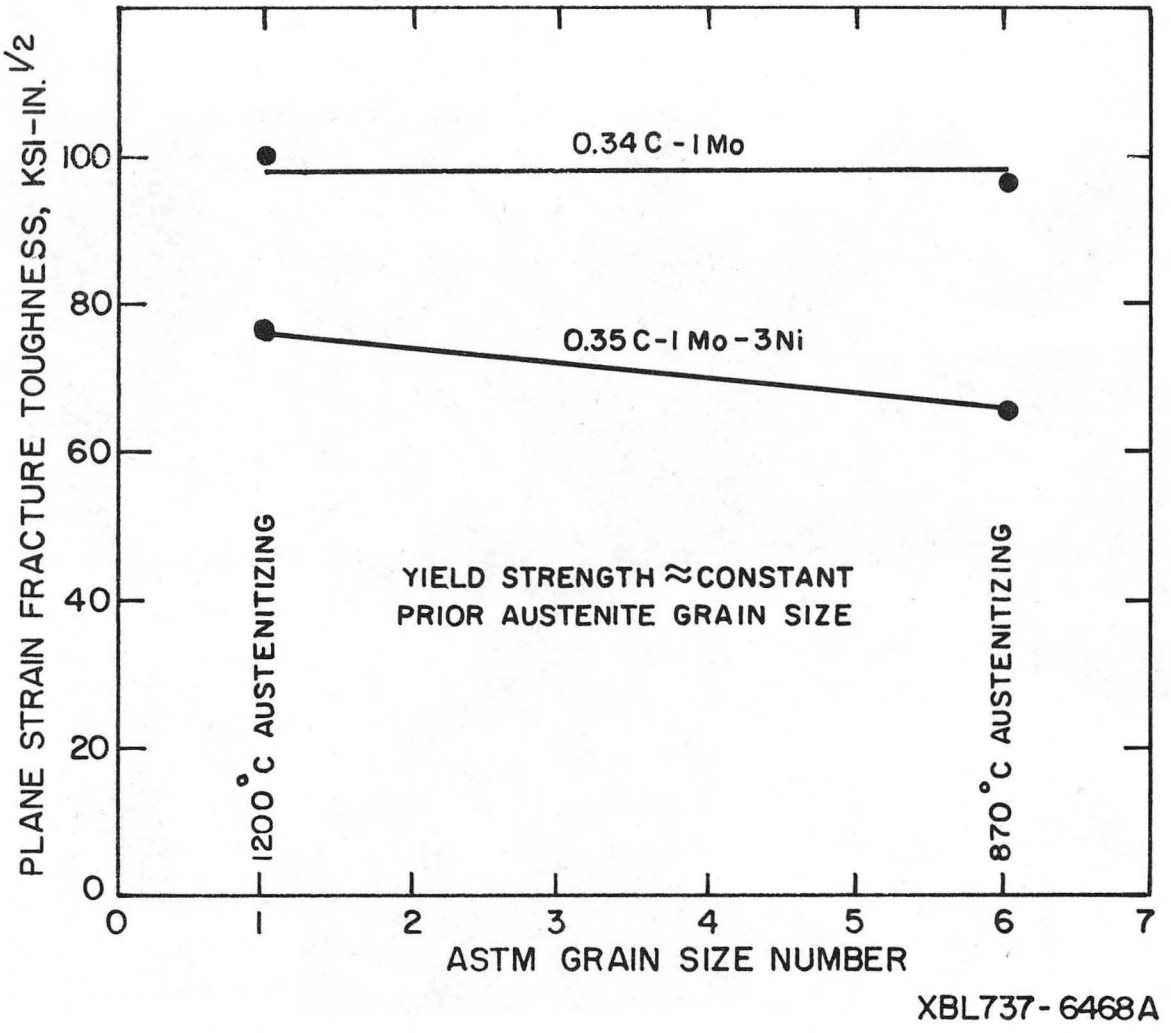

Fig. 2

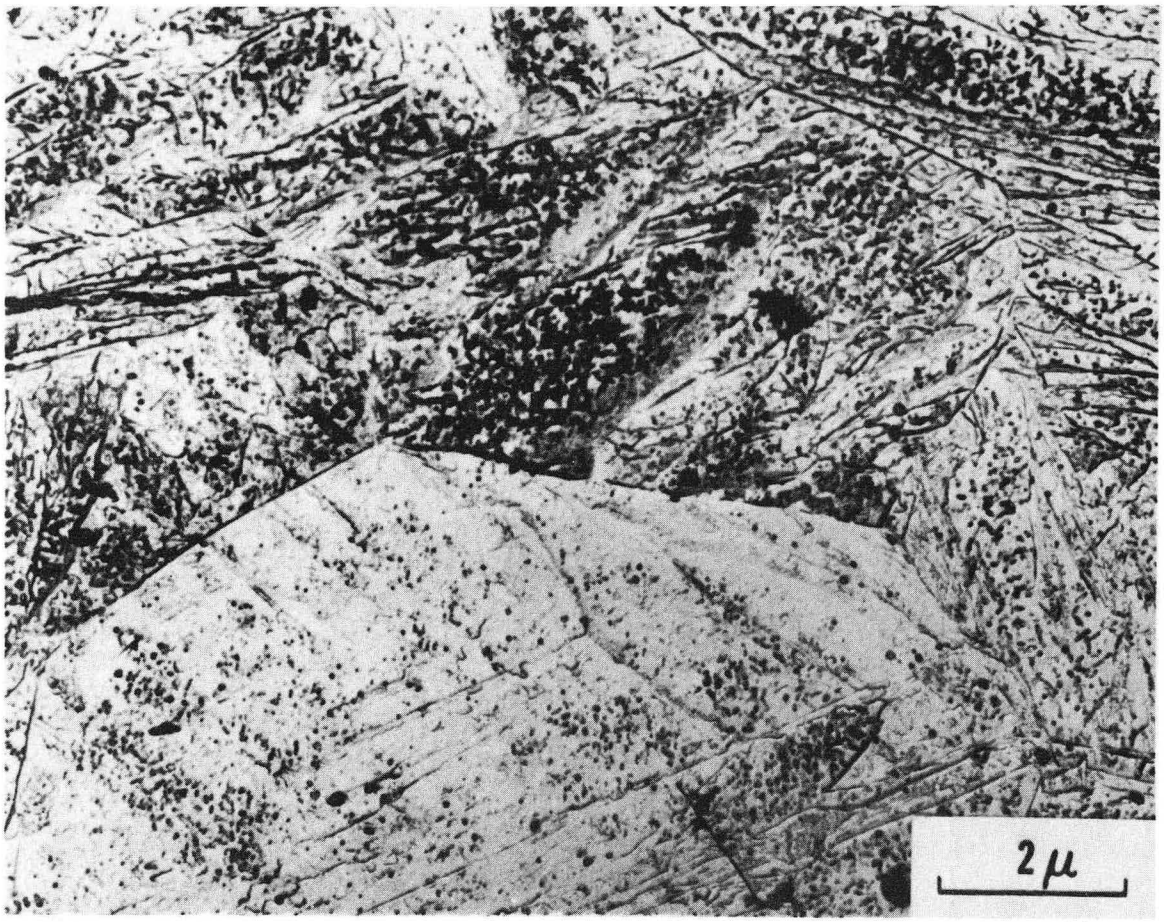

XBB 737-4410

Fig. 3

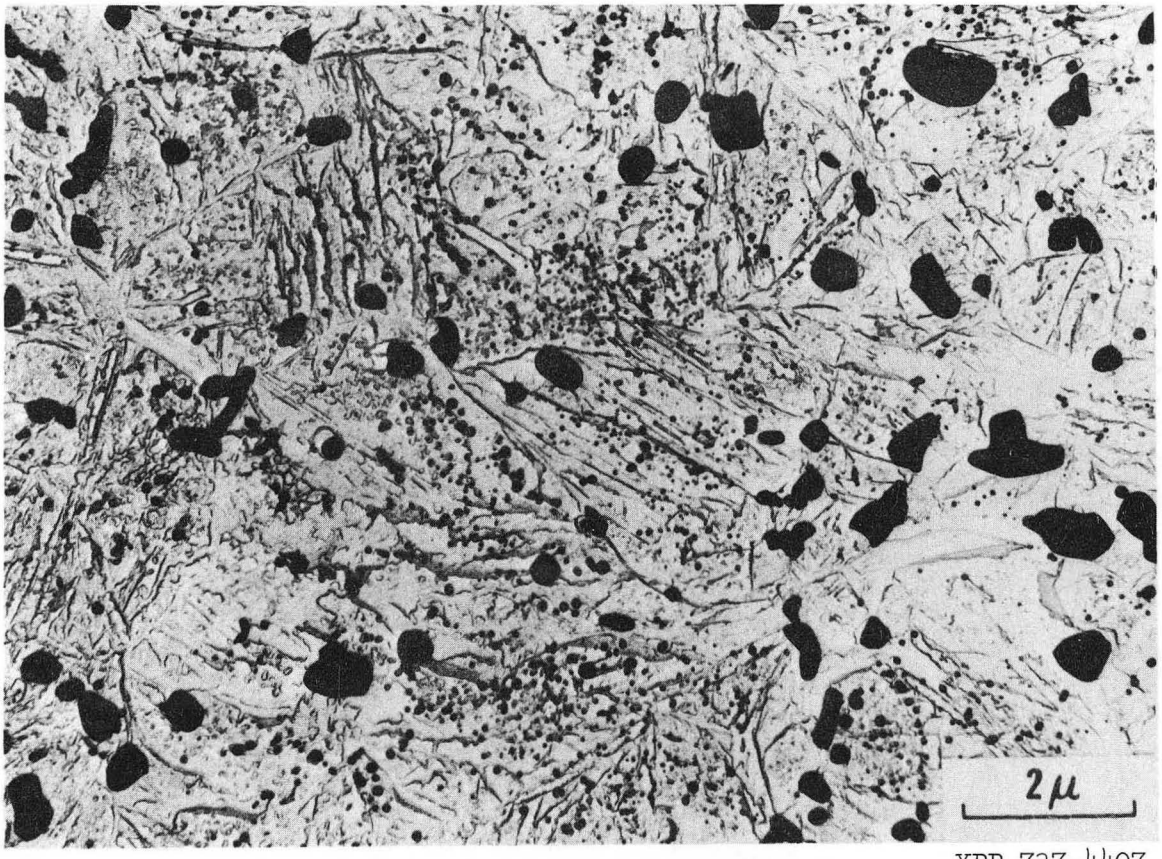

XBB 737-4407

Fig. 4

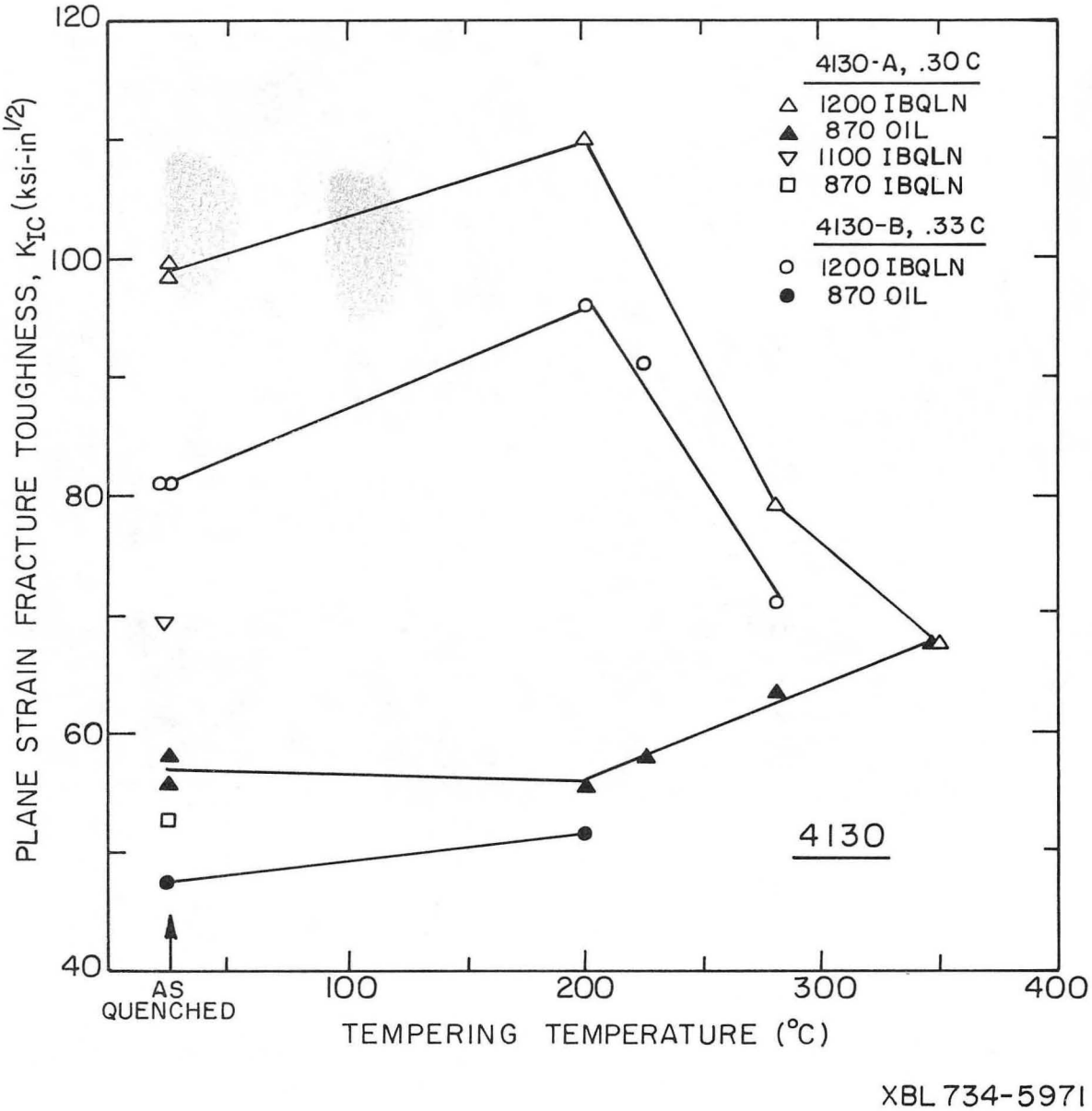
120
100
80
60
40
PLANE STRAIN FRACTURE TOUGHNESS, K_{IC} (ksi-in$^{1/2}$)
4130-A, .30 C
1200 IBQLN
870 OIL
1100 IBQLN
870 IBQLN
4130-B, .33 C
1200 IBQLN
870 OIL
4130
AS QUENCHED
100
200
300
400
TEMPERING TEMPERATURE (°C)
XBL 734-5971

Fig. 5

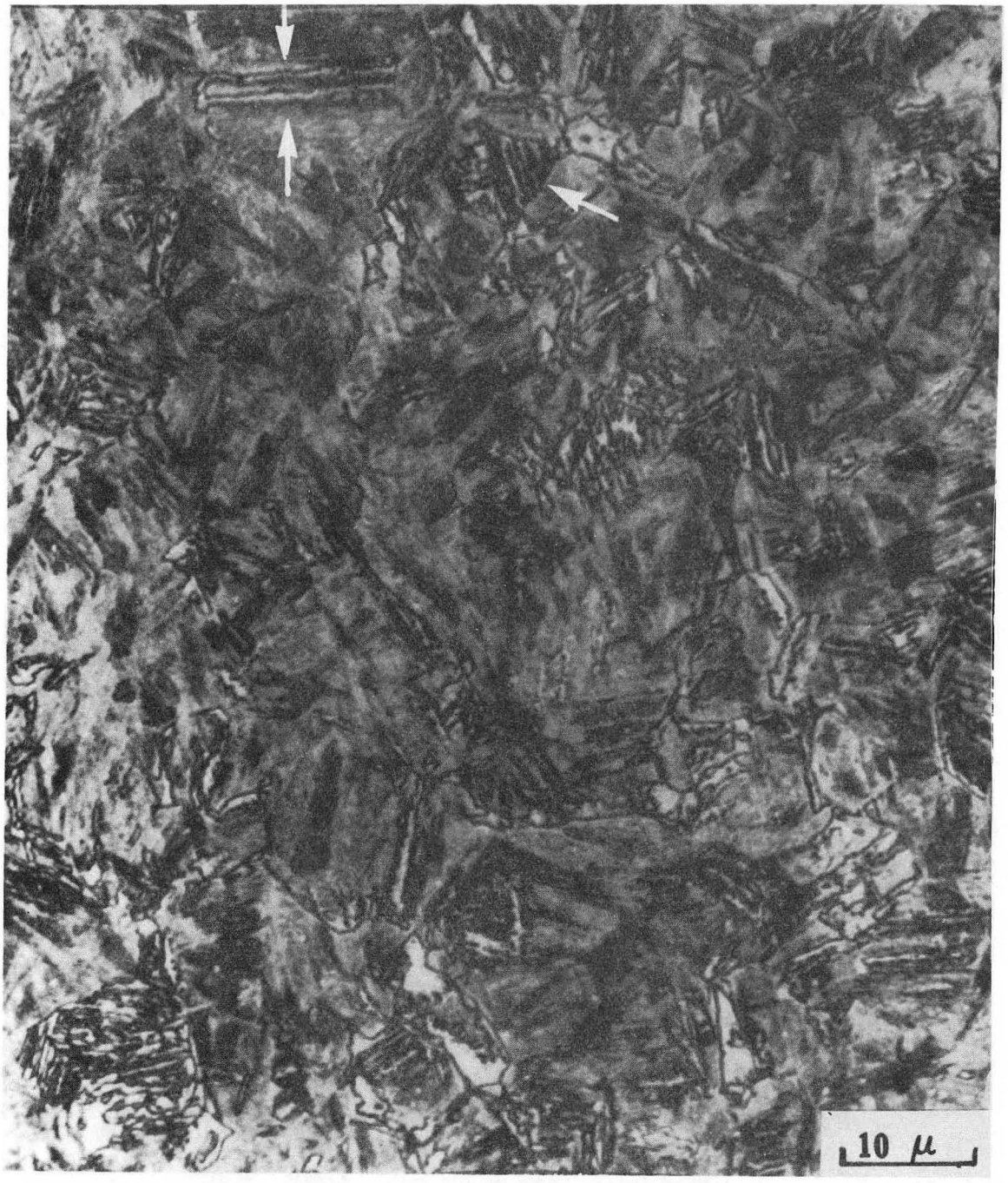

XBB 732-658

Fig. 6(a)

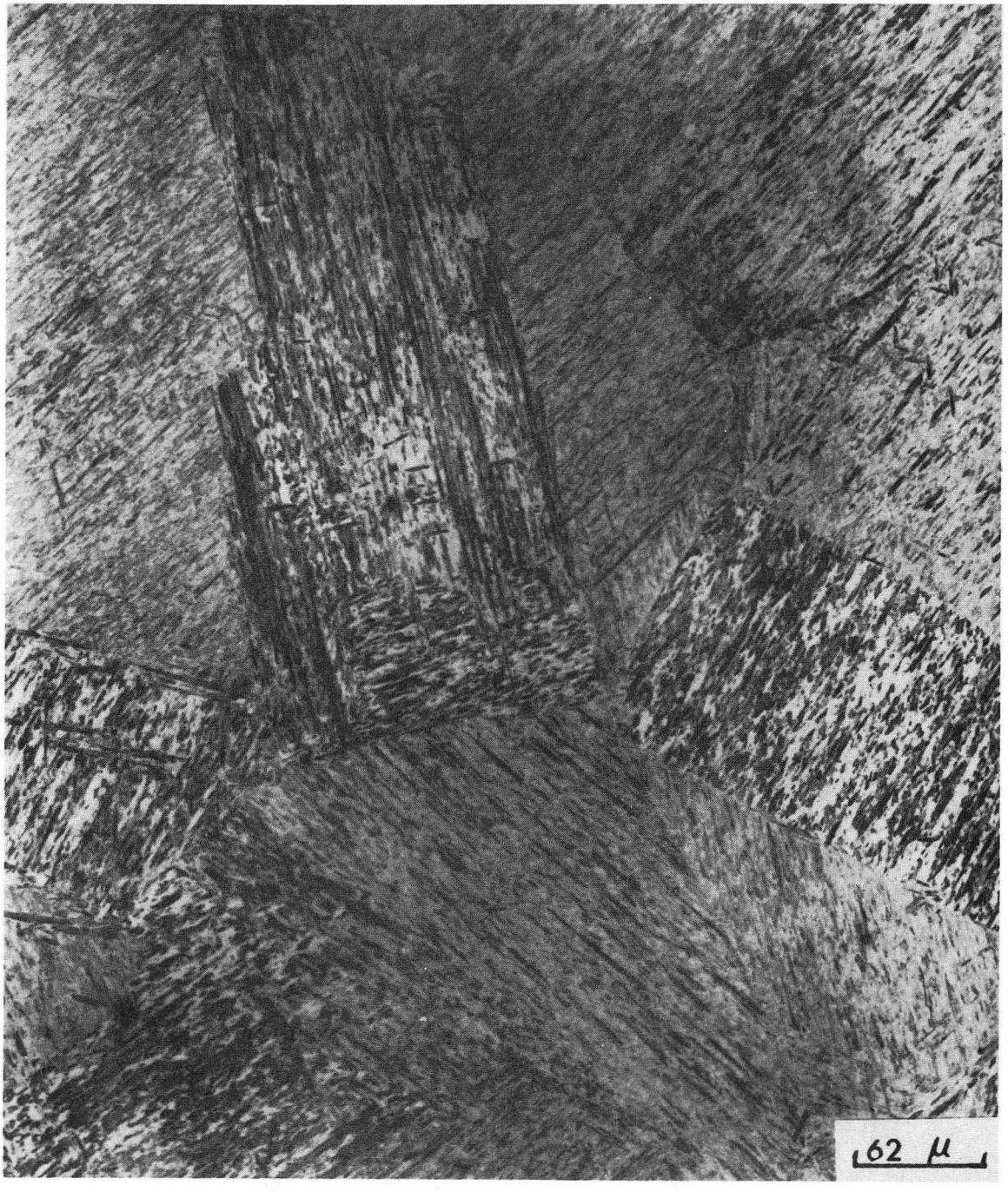

XBB 732-620

Fig. 6(b)

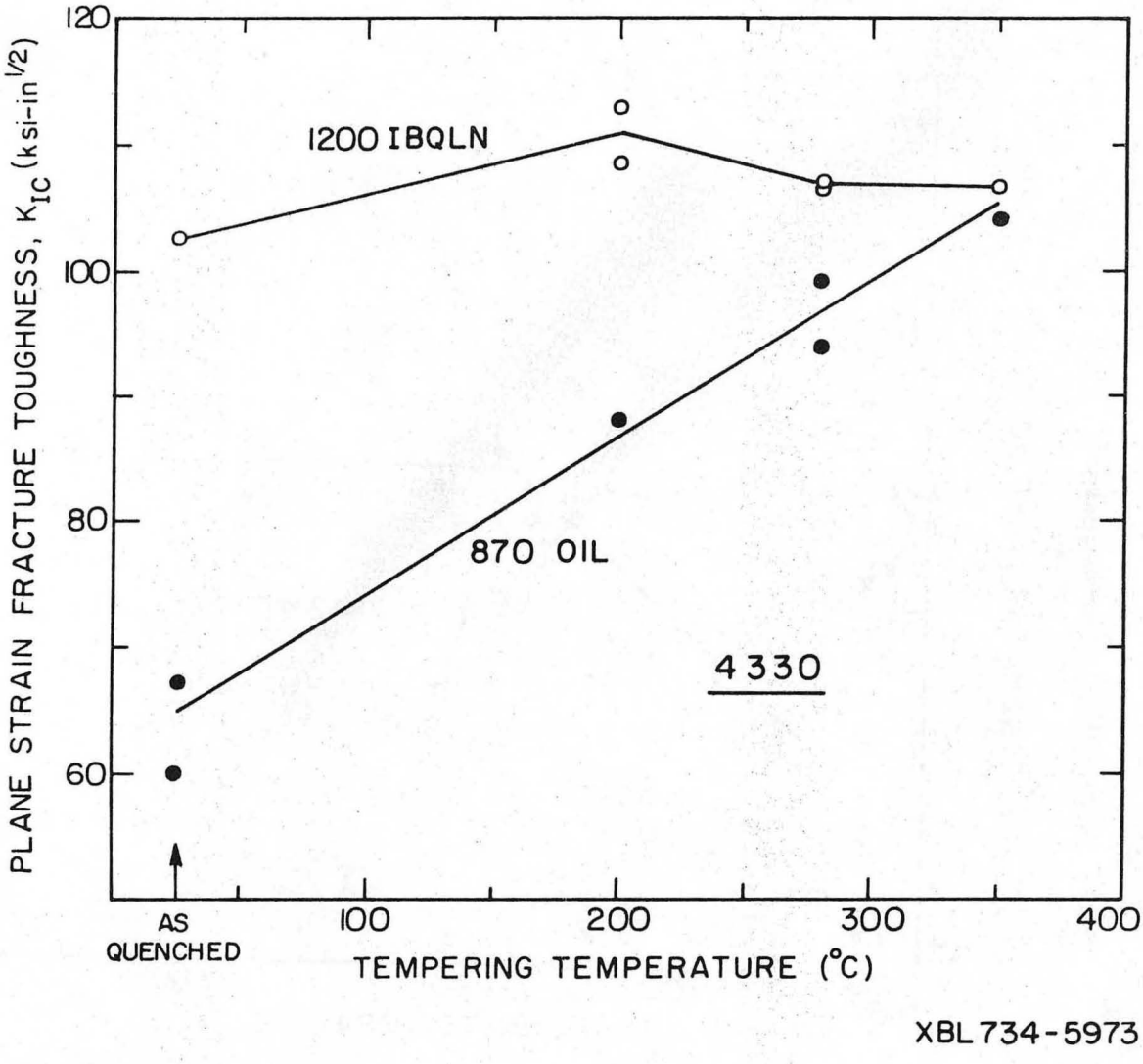

Fig. 7

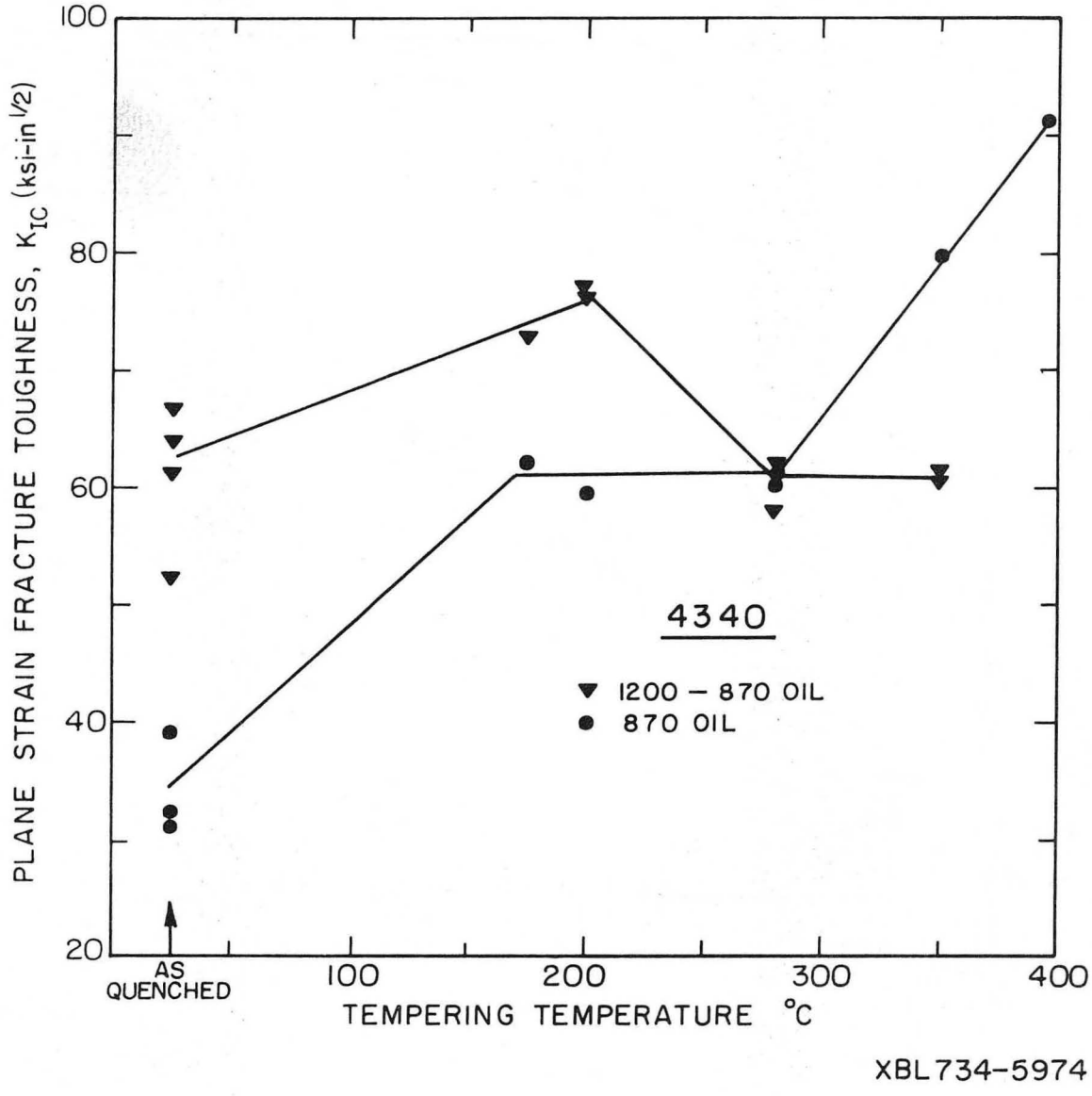
PLANE STRAIN FRACTURE TOUGHNESS, K_{IC} (ksi-in$^{1/2}$)
100
80
60
40
20
AS QUENCHED
100
200
300
400
TEMPERING TEMPERATURE °C
4340
1200 – 870 OIL
870 OIL
XBL734-5974

Fig. 8

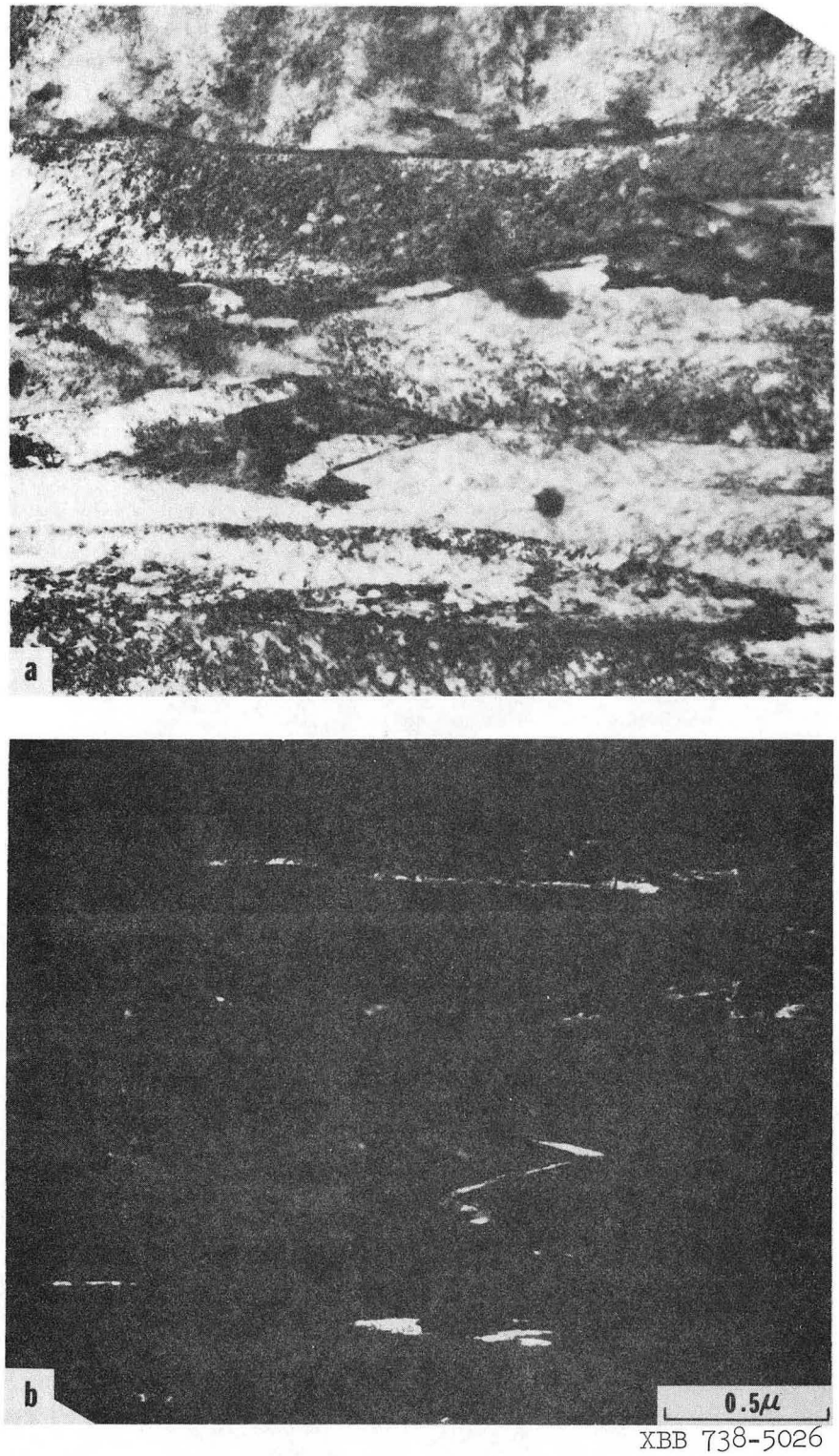

XBB 738-5026

Fig. 9

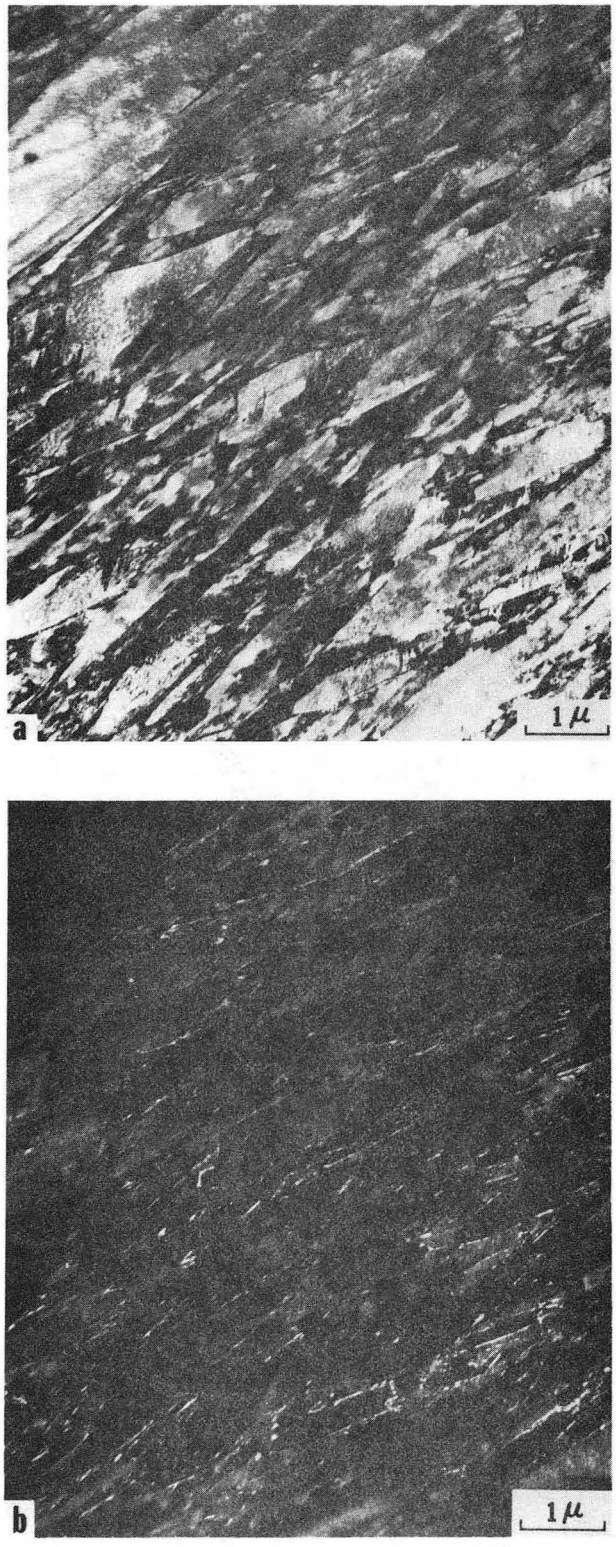

XBB 738-5025

Fig. 10

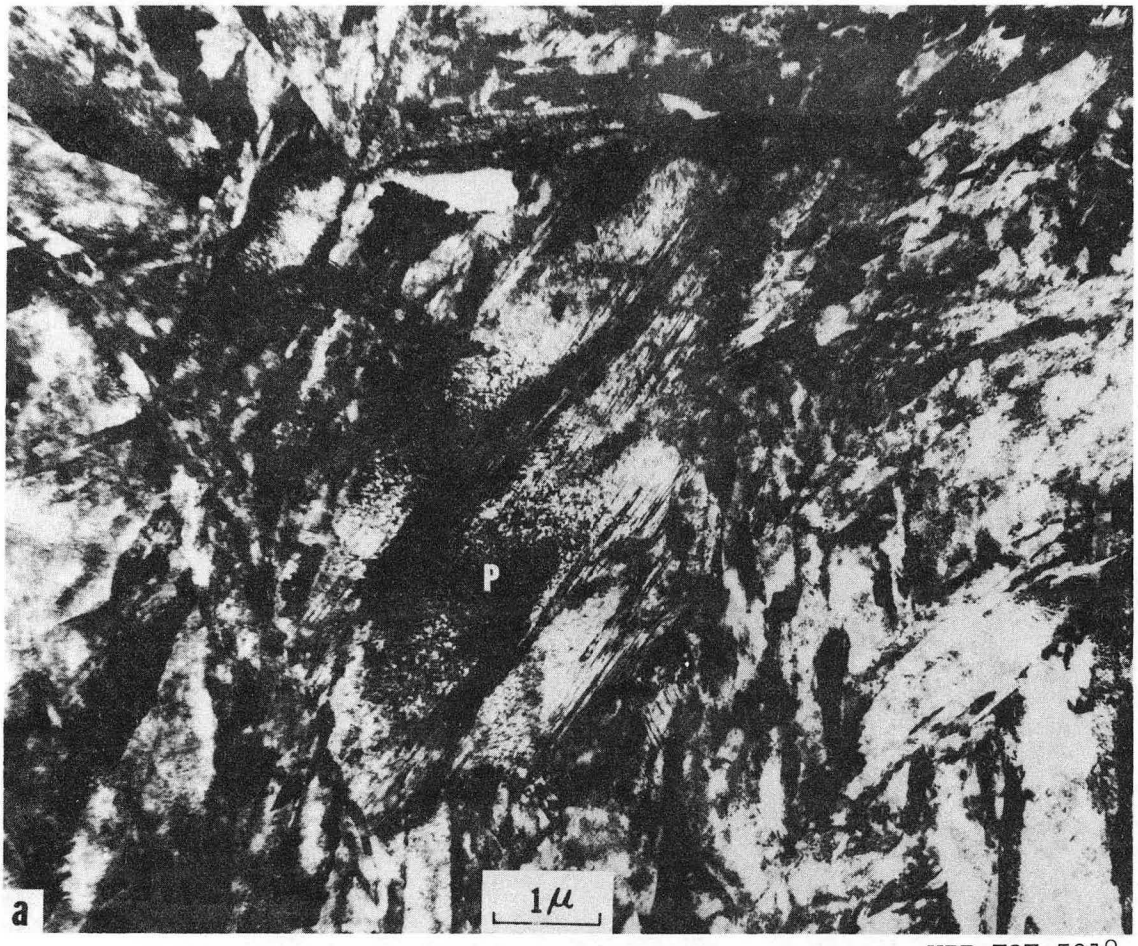

XBB 737-5018

Fig. 11(a)

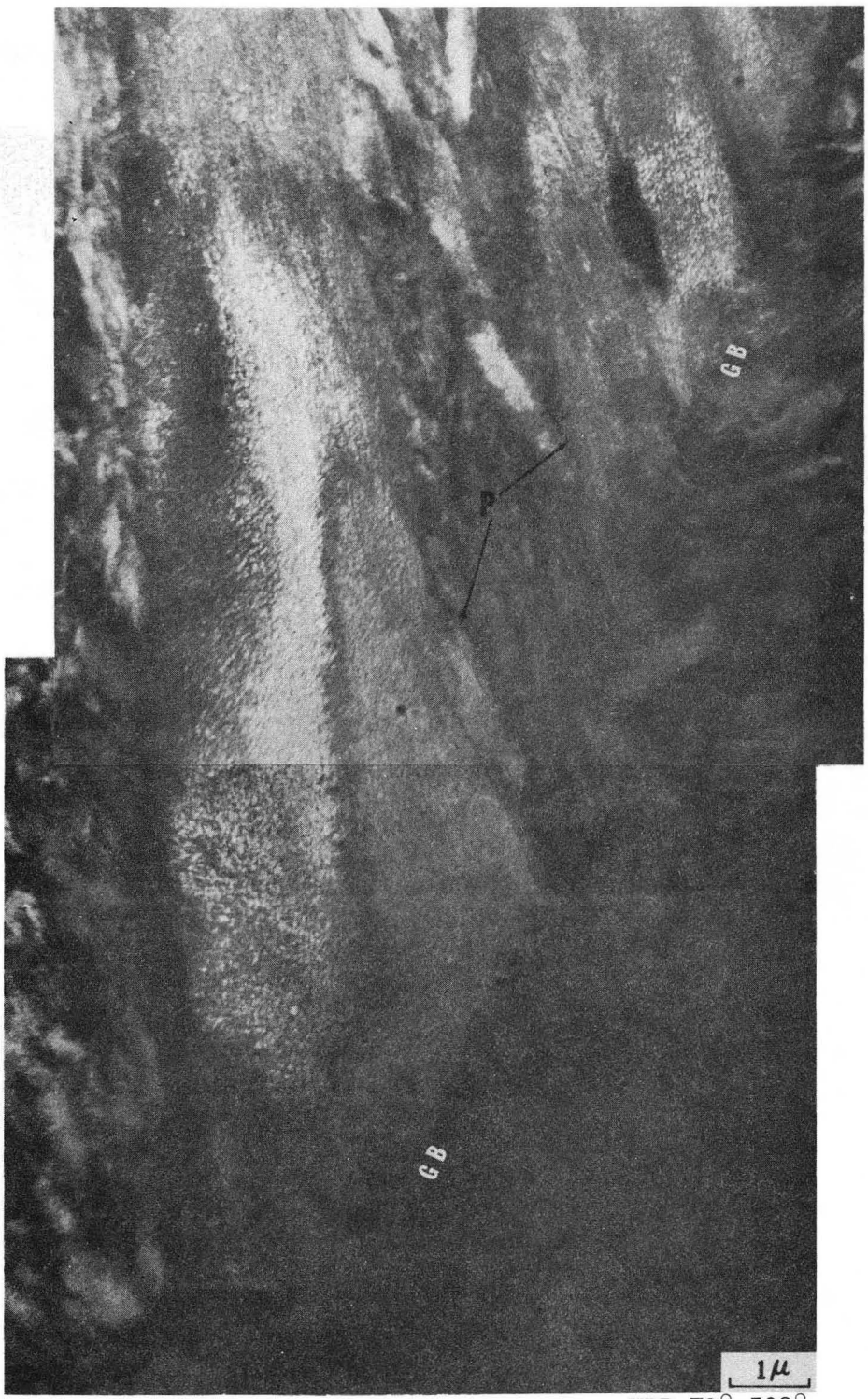

XBB 738-5028

Fig. 11(b)

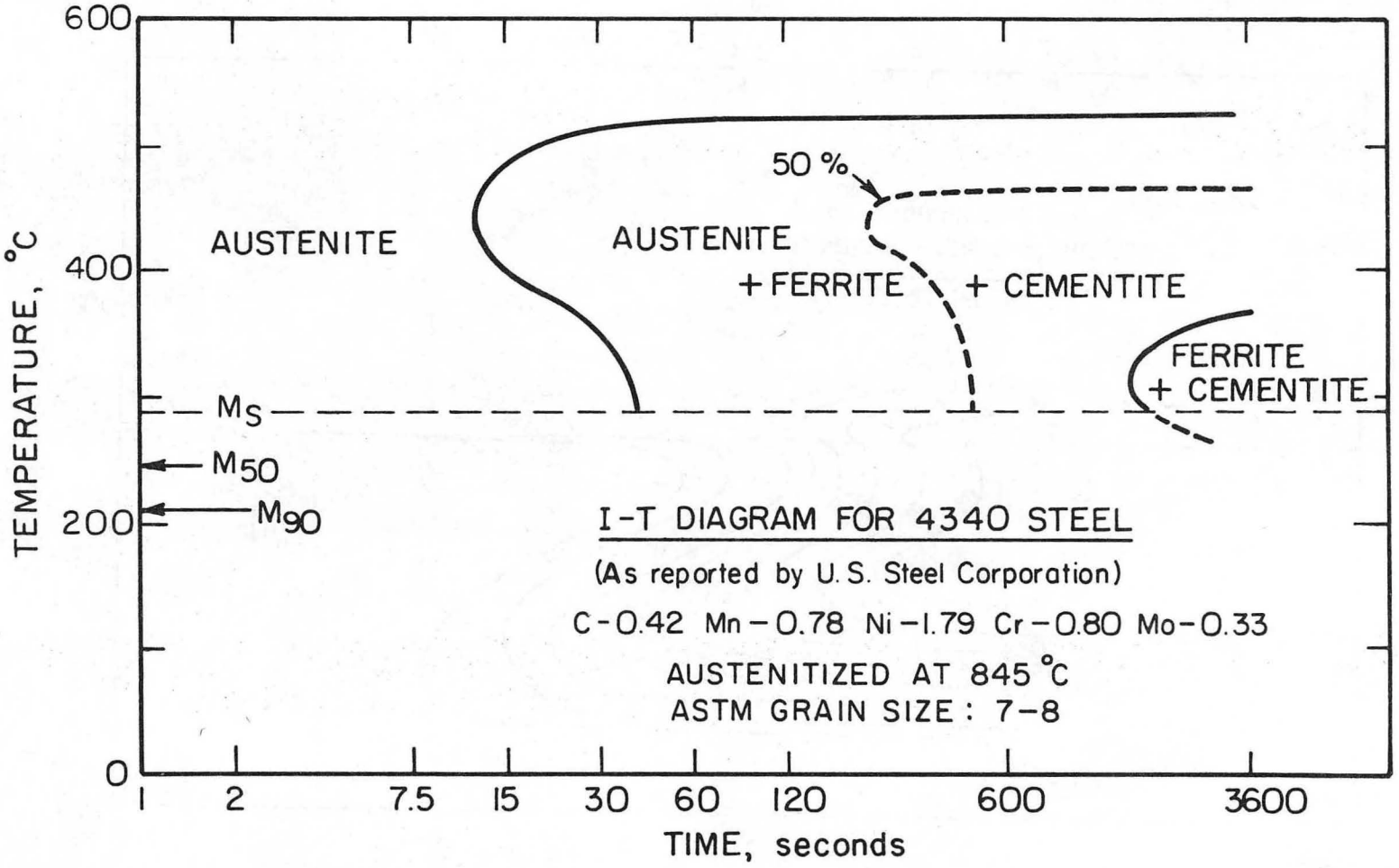

XBL 745-6289

Fig. 12(a)

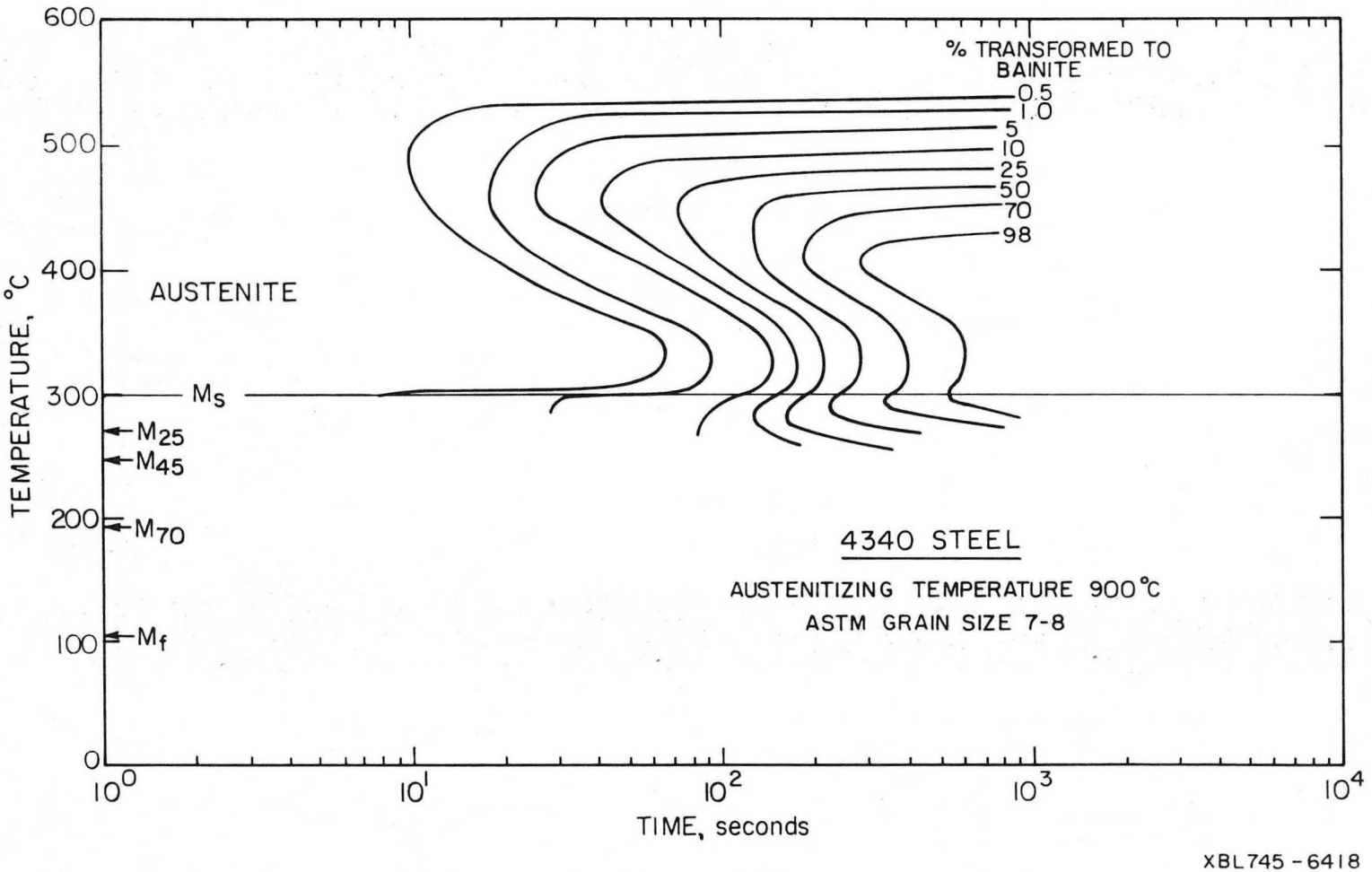
600
500
400
300
200
100
0
TEMPERATURE, °C
% TRANSFORMED TO BAINITE
0.5
1.0
5
10
25
50
70
98
AUSTENITE
M_S
M_{25}
M_{45}
M_{70}
M_f
4340 STEEL
AUSTENITIZING TEMPERATURE 900°C
ASTM GRAIN SIZE 7-8
10^0
10^1
10^2
10^3
10^4
TIME, seconds
XBL745-6418

Fig. 12(b)

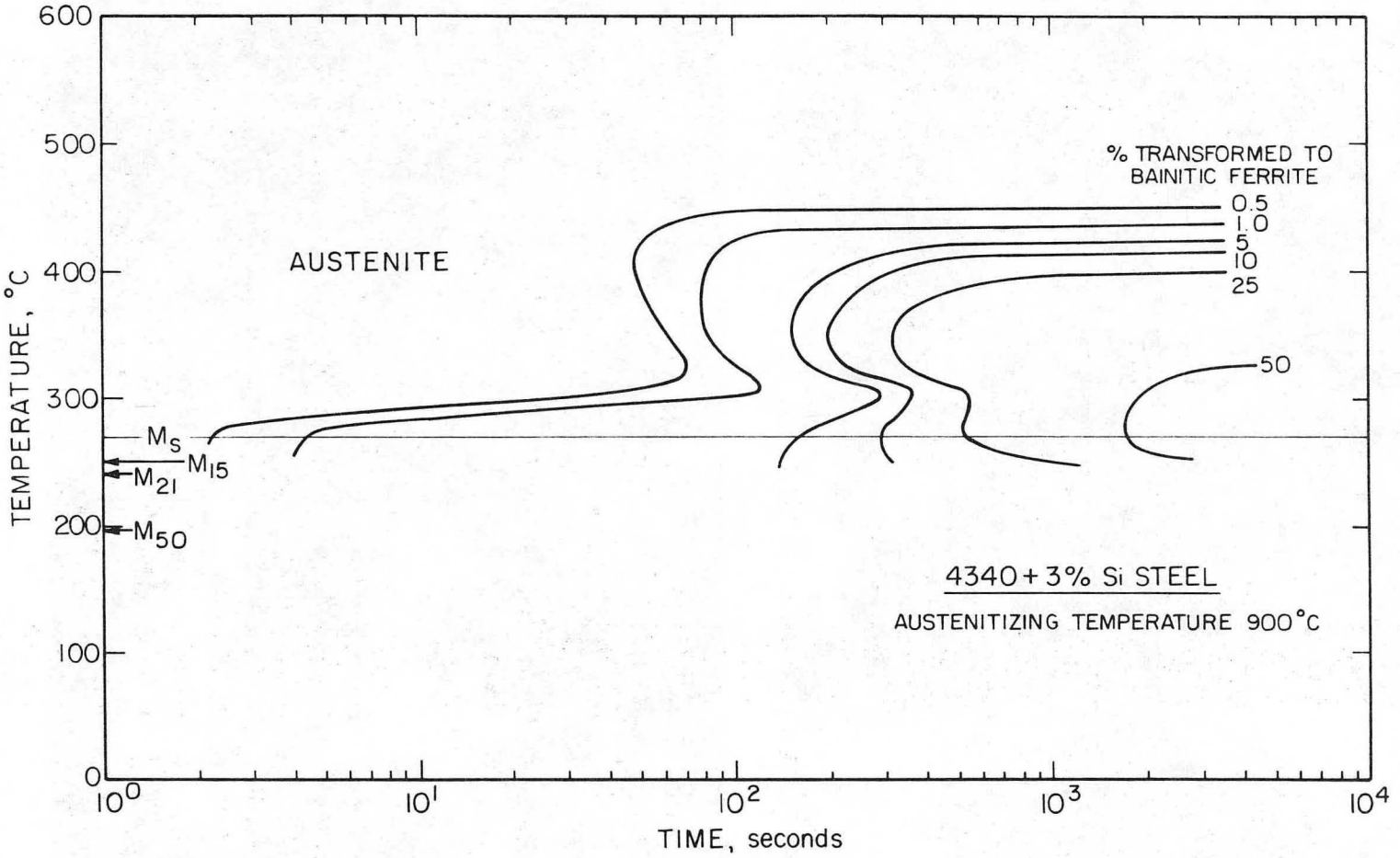

Fig. 13

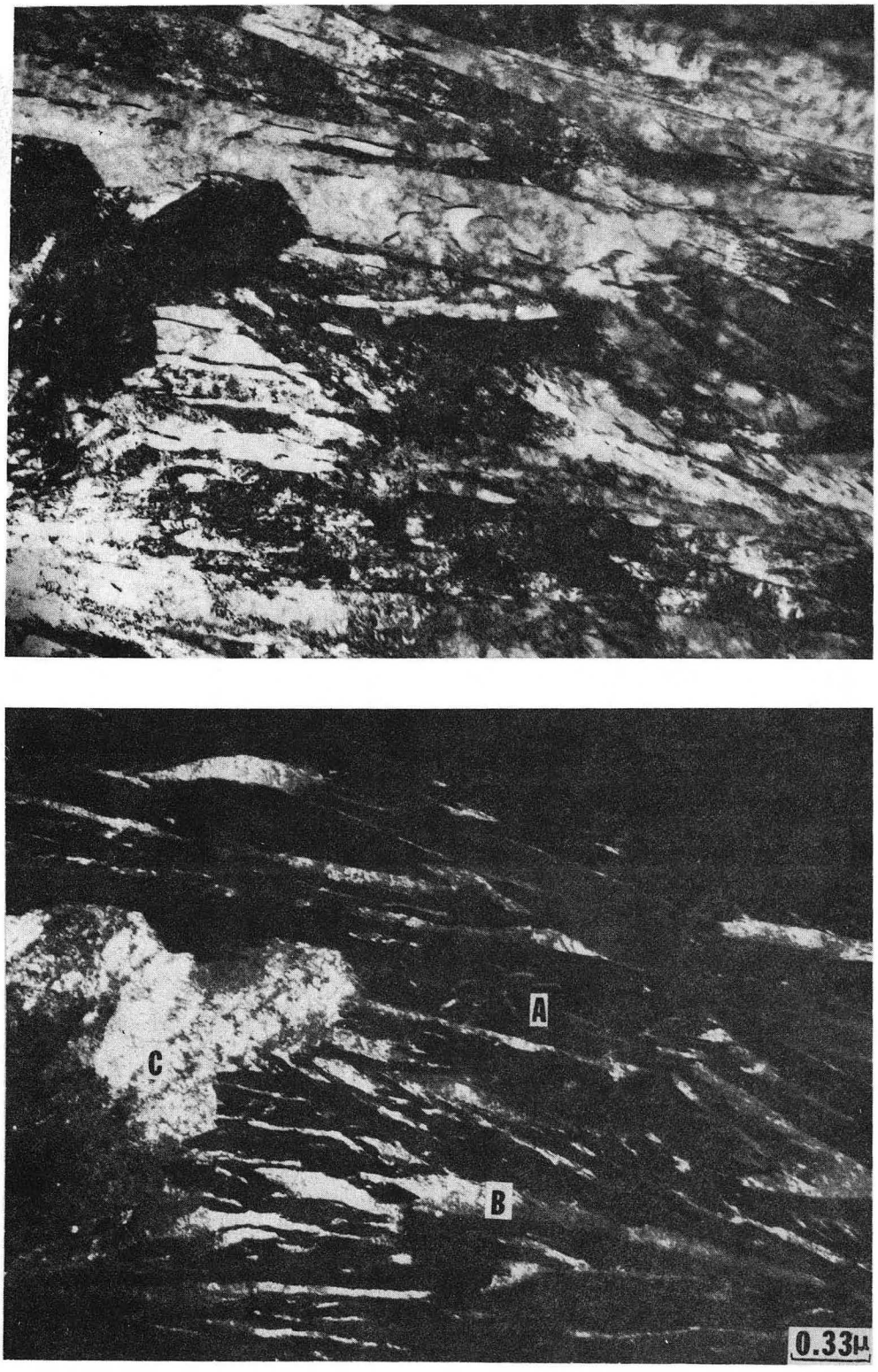

XBB 746-4189

Fig. 14

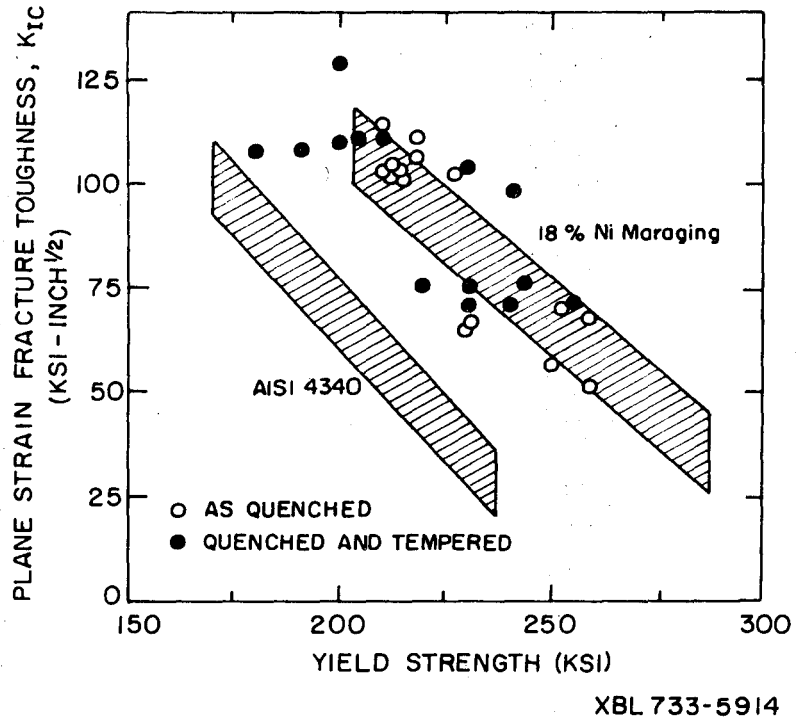

Fig. 15

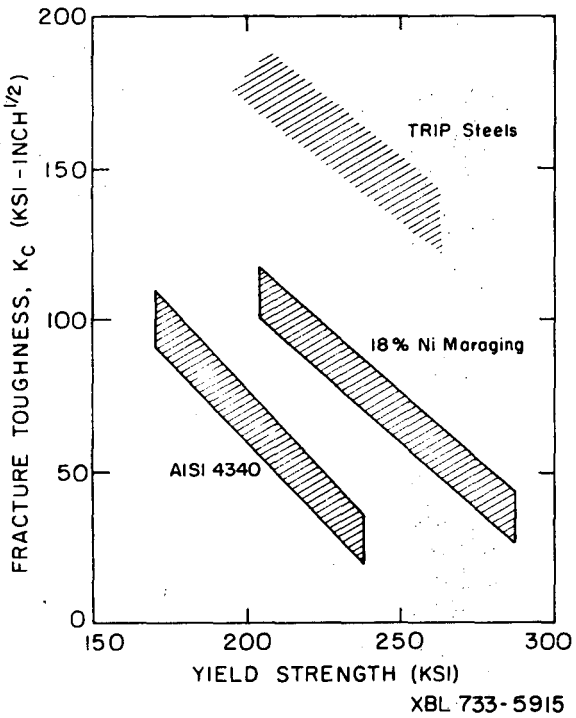
200
150
100
50
0
FRACTURE TOUGHNESS, K_C (KSI-INCH$^{1/2}$)
TRIP Steels
18% Ni Maraging
AISI 4340
150
200
250
300
YIELD STRENGTH (KSI)
XBL 733-5915

Fig. 16

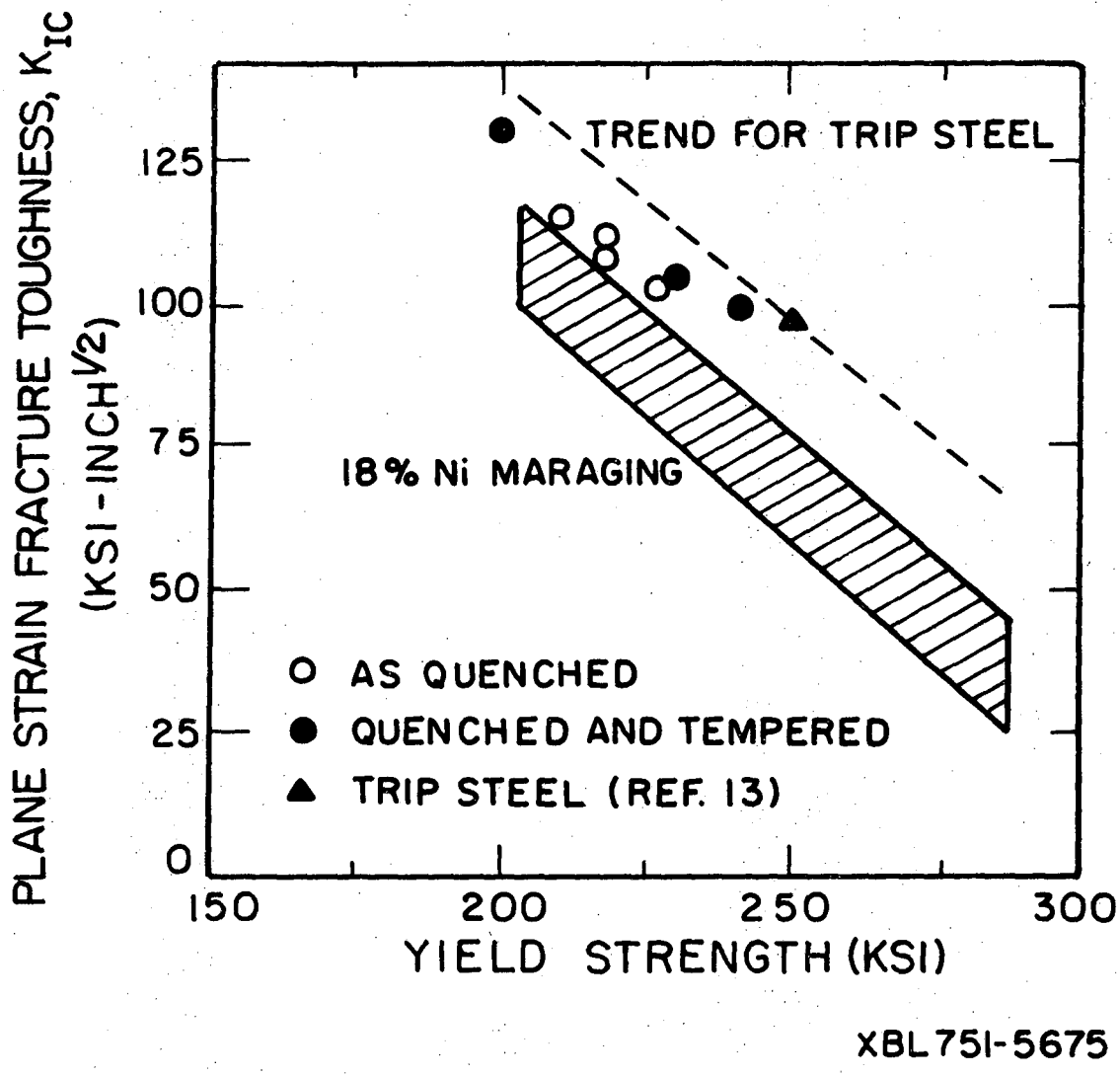
PLANE STRAIN FRACTURE TOUGHNESS, K_{IC}
(KSI-INCH$^{1/2}$)
125
100
75
50
25
0
150
200
250
300
YIELD STRENGTH (KSI)
TREND FOR TRIP STEEL
18% Ni MARAGING
AS QUENCHED
QUENCHED AND TEMPERED
TRIP STEEL (REF. 13)
XBL751-5675

Fig. 17

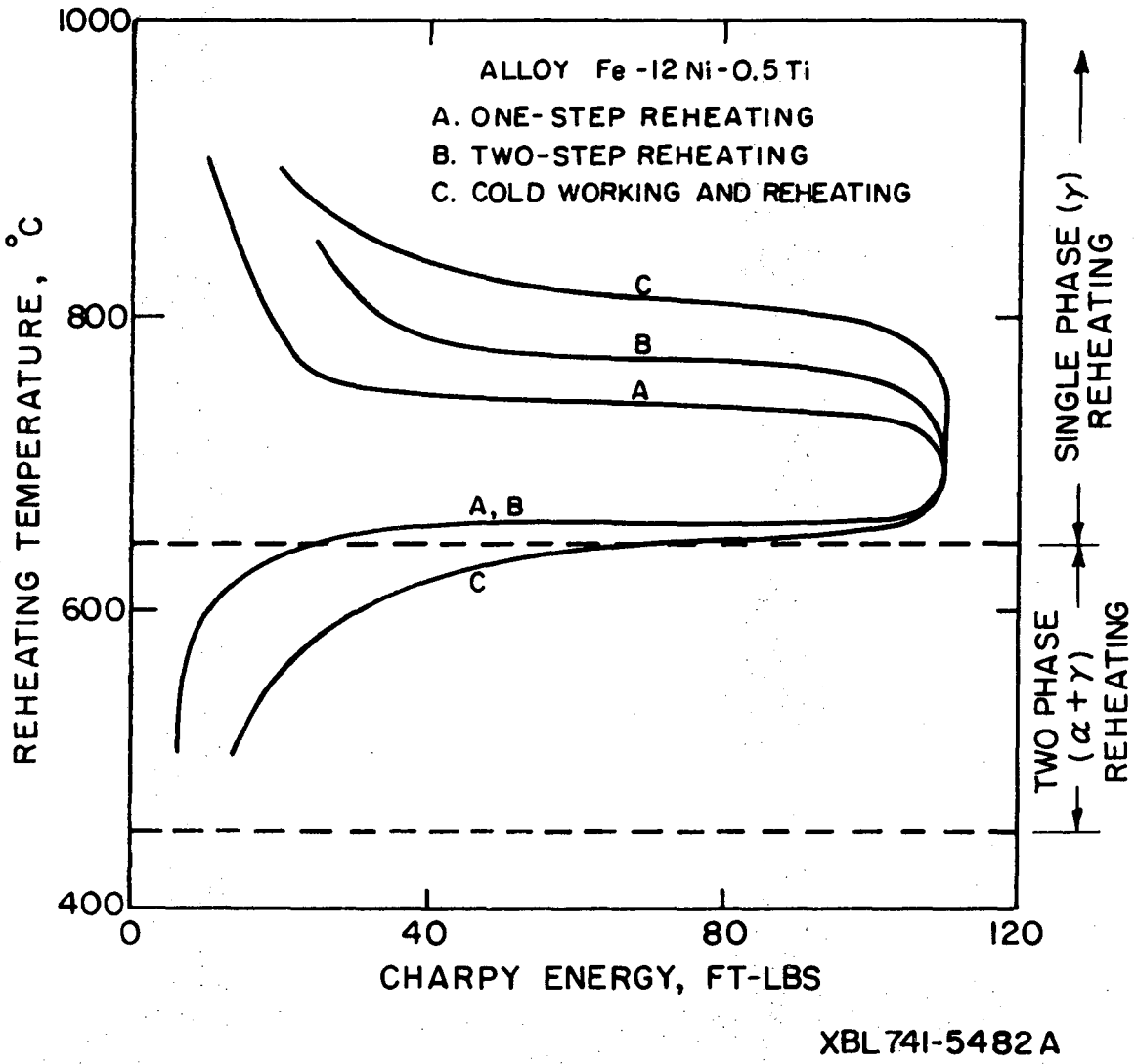
ALLOY Fe -12 Ni-0.5 Ti
A. ONE-STEP REHEATING
B. TWO-STEP REHEATING
C. COLD WORKING AND REHEATING
REHEATING TEMPERATURE, °C
1000
800
600
400
0
40
80
120
CHARPY ENERGY, FT-LBS
C
B
A
A, B
C
SINGLE PHASE (γ) REHEATING
TWO PHASE (α+γ) REHEATING
XBL 741-5482 A

Fig. 18

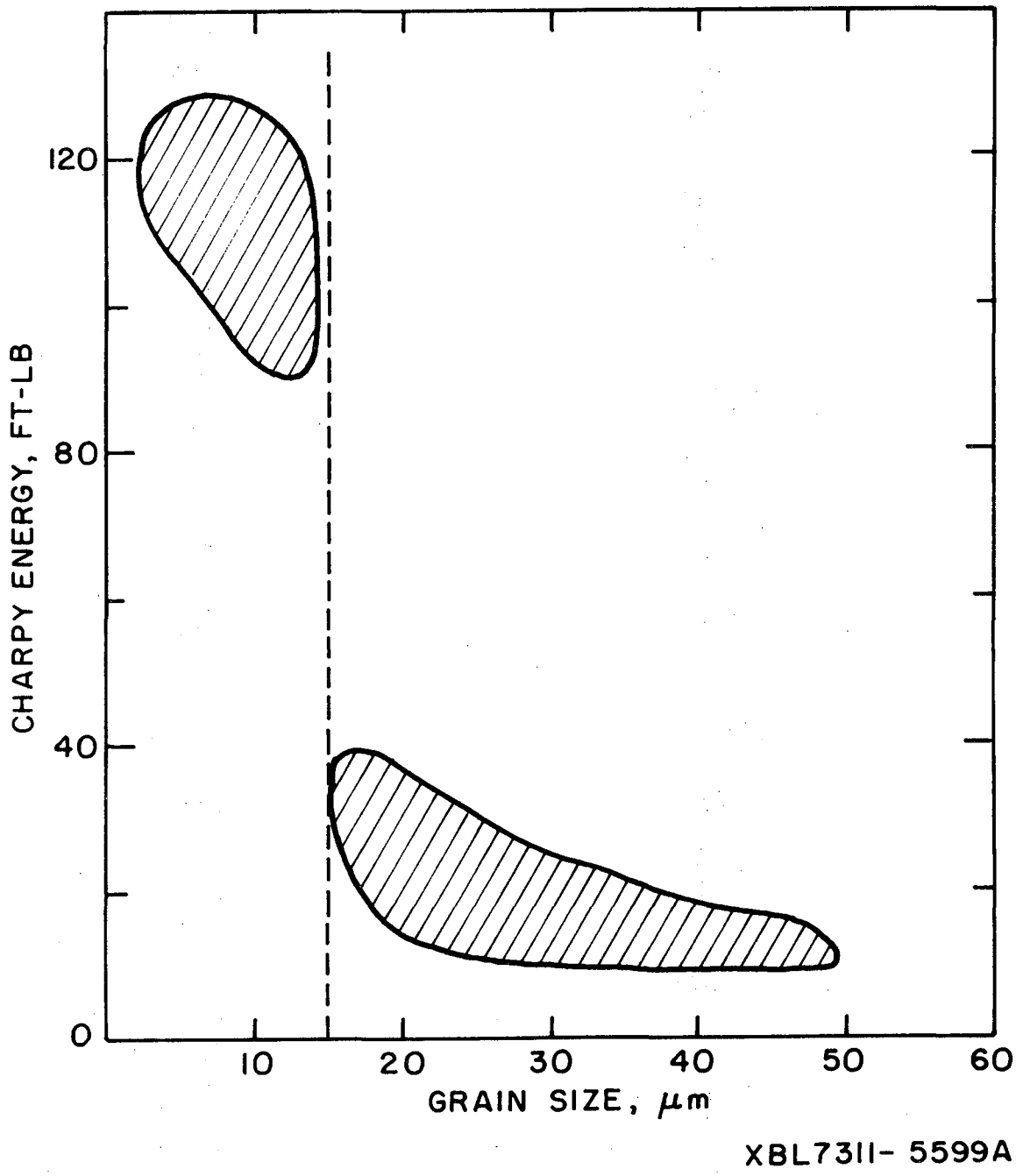
120
80
40
0
CHARPY ENERGY, FT-LB
10
20
30
40
50
60
GRAIN SIZE, μm
XBL7311- 5599A

Fig. 19

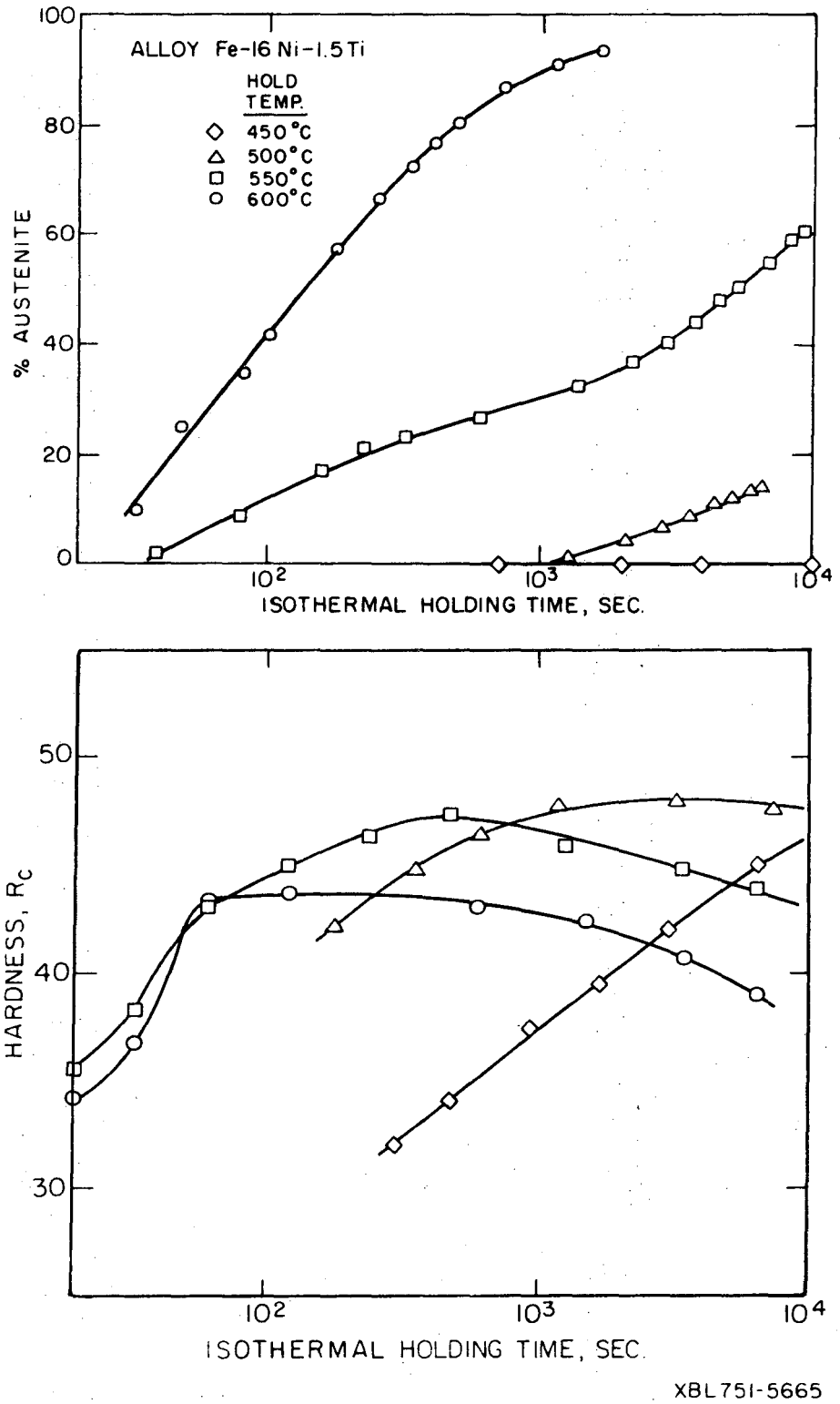
ALLOY Fe-16 Ni-1.5 Ti
HOLD TEMP.
450°C
500°C
550°C
600°C
% AUSTENITE
ISOTHERMAL HOLDING TIME, SEC.
A
HARDNESS, R_c
ISOTHERMAL HOLDING TIME, SEC.
B
XBL751-5665

Fig. 20

TECHNICAL INFORMATION DIVISION
LAWRENCE BERKELEY LABORATORY
UNIVERSITY OF CALIFORNIA
BERKELEY, CALIFORNIA 94720